CHALMERS
UNIVERSITY OF TECHNOLOGY

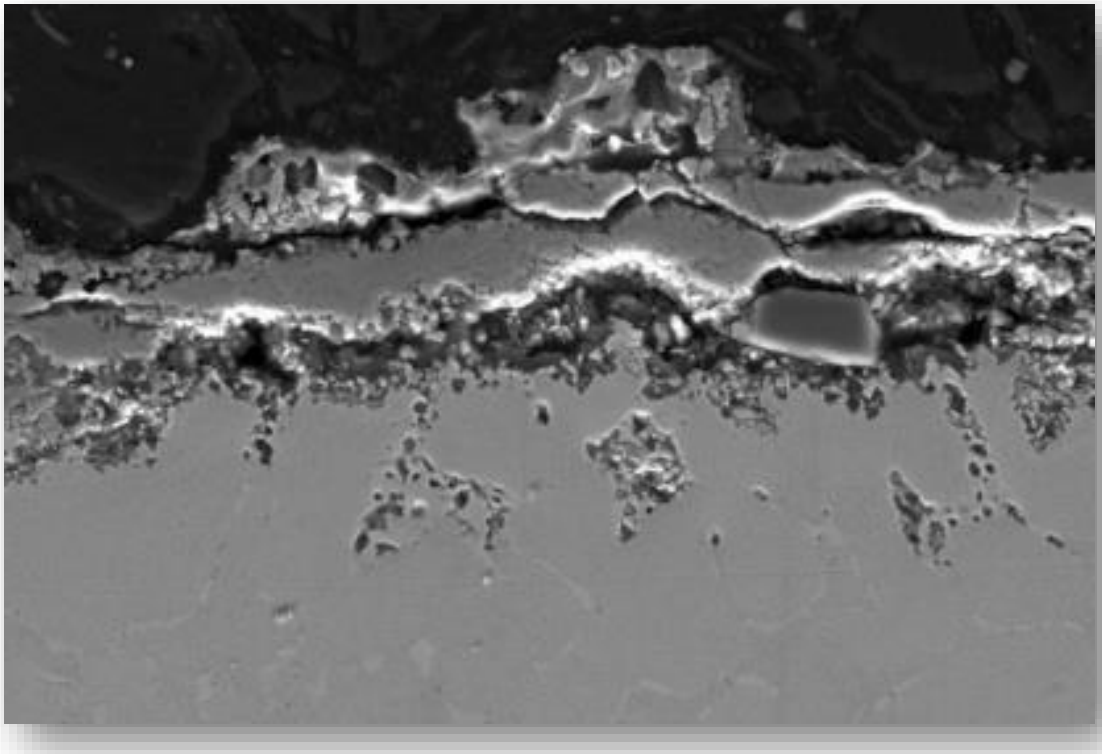

Surface characterization and grinding of Duplex 2205 Stainless Steel slabs

Master's thesis in Production Engineering

Ari Ahmad

DEPARTMENT OF INDUSTRIAL AND MATERIALS SCIENCE

CHALMERS UNIVERSITY OF TECHNOLOGY
Gothenburg, Sweden 2025
www.chalmers.se

Master’s Thesis 2025

Surface characterization and grinding of Duplex 2205 Stainless Steel slabs

ARI AHMAD

CHALMERS
UNIVERSITY OF TECHNOLOGY

Department of Industrial and Materials Science
CHALMERS UNIVERSITY OF TECHNOLOGY
Göteborg, Sweden 2025

Surface characterization and grinding of Duplex 2205 stainless steel slabs
Ari Ahmad

Supervisor: Anders Groth
Examiner: Gustav Holmqvist

Cover: Oxide/casting powder mixture present in the bulk

Department of Industrial and Materials Science
Chalmers University of Technology
SE-412 96 Göteborg, Sweden
Telephone + 46 (0)31-772 1000

Gothenburg, Sweden 2025

Abstract

This study investigates the optimization of grinding processes for duplex 2205 stainless steel slabs at Outokumpu Avesta works. The primary objective is to analyze and enhance these processes to achieve cost reductions, increased productivity, and improved material processing efficiency. To fulfill this aim, a combination of theoretical analysis and practical experiments has been conducted, with a particular focus on the effects of different grinding methods on oxidation levels and surface quality.

Through the evaluation of various grinding conditions, the study identifies opportunities for process improvements that can enhance production efficiency. It is shown that implementing coarse grindings process only can reduce total material loss by 21 ton, decrease grinding time by 200 hours, and result in potential savings of 40% in grinding wheel costs during the reference period. The findings highlight the need to balance cost-effectiveness, product quality, and environmental considerations. This work aims to support Outokumpu's long-term development strategy while contributing to the company's competitiveness in the global market.

Table of Contents

Abstract **5**

Preface **8**

List of Acronyms **9**

Nomenclature **10**

List of figures **11**

List of Tables **13**

1. Introduction **1**

1.1 Background *1*

1.2 Purpose *2*

1.3 Research Questions *2*

1.4 Delimitations *2*

1.5 Company *3*

1.5.1 Historical Development of Avesta Works 3

1.5.2 Avesta's Role within Outokumpu 3

1.5.3 General Process Route 3

2. The Steel Grade in This Study **6**

2.1 Stainless Steel Groups in General *6*

2.2 What is Duplex Stainless Steel? *8*

2.3 Duplex 2205 Stainless steel *9*

2.3.1 Chemical Properties 9

2.3.2 Corrosion Resistance 9

2.3.3 Heat Resistance 9

2.3.4 Heat Treatment 10

2.3.5 Machining – Mechanical Processing 10

3 Grinding **11**

3.1 The Origin and Development of Grinding *11*

3.2 What is Grinding? *11*

3.3 Composition of grinding tool *11*

3.4 Grinding Methods *12*

3.5 Work Materials *13*

3.6 Contact Geometry *14*

3.7 Grinding Forces: *15*

3.8 Aggressiveness in Cold Grinding Processes: *15*

4 Grinding Production **17**

4.1 Grinding Process *17*

4.2 The Material Removal Process *18*

4.3 Grinding process routes at Avesta Works *19*

4.4 Cold grinding process routes at Avesta Works *21*

5 Surface Roughness and Its Parameters 23

5.1 What is Roughness? *23*

5.2 Why is Roughness Important? ..... ***Error! Bookmark not defined.***

5.3 Workpiece surface measurement *23*

5.3.1 Basis for evaluation 23

5.3.2 Arithmetic Mean Roughness (Ra) 24

5.3.3 Maximum Roughness Profile Height (Rz) 24

5.3.4 Total profile height (Rt) 25

6 Methods and experimentation 26

6.1 Slab Dimensions *26*

6.1.1 Nominal slab dimensions in the cold state ..... **Error! Bookmark not defined.**

6.2 Grinding Tests *27*

6.2.1 Surface Roughness Measurement Method 28

6.3 Slab sample preparation: *30*

6.4 Metallographic Sample Preparation *34*

7 Results 37

7.1 Surface Roughness Measurements of Production Slabs: *37*

7.2 Surface Roughness with New Cold Grinding Methods *38*

7.3 Analysis of cross sections *40*

7.3.1 The cross section from a cast (non-ground) surface 40

7.3.2 Oxide/casting powder composition on the Duplex 2205 slab surface (cast surface) 42

7.3.3 Surface Analysis of hot ground surface 49

7.3.4 Surface Analysis of Hot + Cold ground surface sample 53

7.4 Optimization of the Grinding Process *57*

7.5 Time and Material Savings *60*

7.6 Results from Cold Rolling: *62*

8 Discussion 63

9 Conclusions 64

10 Suggestions for future work 65

11 References 66

Appendix 69

Preface

This thesis was conducted between August 2024 and January 2025 at Outokumpu in collaboration with Chalmers University of Technology. The work has focused on surface characterization and grinding of Duplex 2205 stainless steel slabs as part of the steel mill's operations.

I would like to express my gratitude to my supervisor, Anders Groth, for his support and guidance throughout this project.

My sincere appreciation goes to my examiner, Gustav Holmqvist, for his constructive feedback and valuable suggestions, which have contributed to improving the quality of this thesis.

Special thanks are also extended to all colleagues at the Cold Grinding department, whose experience and knowledge have been invaluable to my understanding of both theoretical and practical applications.

Finally, I would like to thank my family, my girlfriend Ronahi, and my friends for their support and encouragement throughout my studies.

Ari Ahmad

Avesta, the 17^{th} of Dec 2024

List of Acronyms

The following is a comprehensive alphabetical list of acronyms utilized throughout this thesis:

KBR	Cold Rolling Mill
L-76	Annealing and Pickling
Z-High	Cold Rolling
S-13	Finishing Line
LOM	Light Optical Microscopy
SEM	Scanning Electron Microscopy

Nomenclature

$\boldsymbol{\mu}$	The coefficient of friction
$\boldsymbol{d_s}$	Diameter
$\boldsymbol{v_s}$	Peripheral speed of the grinding wheel
$\boldsymbol{a_e}$	depth of cut
$\boldsymbol{v_w}$	workpiece linear speed
$\boldsymbol{l_c}$	arc length / contact length
$\boldsymbol{F_T}$	The tangential force
$\boldsymbol{F_N}$	The normal force
$\boldsymbol{Z}$	Depth
$\boldsymbol{k_s}$	Specific cutting force
$\boldsymbol{R_a}$	Arithmetic mean surface roughness
$\boldsymbol{R_z}$	Maximum surface roughness
$\boldsymbol{R_t}$	Total surface roughness
$\boldsymbol{V_c}$	Cutting speed
$\boldsymbol{V_f}$	Feed rate
$\boldsymbol{ap}$	Depth of cut

List of figures

Figure 1 The Process Route at Outokumpu Avesta.
Figure 2 Austenitic microstructure.
Figure 3 Martensitic microstructure.
Figure 4 Ferritic microstructure.
Figure 5 Duplex microstructure.
Figure 6 The Development of Different Types of Duplex Stainless Steels Over Time.
Figure 7 Structure of the Grinding Wheel.
Figure 8 Surface grinding.
Figure 9 The Relationship Between the Workpiece and the Grinding Wheel in Surface Grinding.
Figure 10 Internal Grinding of Cylindrical Components.
Figure 11 Grinding Forces.
Figure 12 90° set up angle.
Figure 13 45° set up angle.
Figure 14 Material removal process.
Figure 15 ploughing, Rubbing and cutting occur as grain penetration progressively increases within the constant arc.
Figure 16 Hot ground slabs ready for cold grinding.
Figure 17 90° grinding in progress.
Figure 18 90° grinding in process.
Figure 19 Slab after cold grinding.
Figure 20 Used grinding wheels.
Figure 21 Measuring lengths.
Figure 22 Arithmetical mean height for a roughness profile.
Figure 23 Maximum height of profile curve for a roughness profile.
Figure 24 Total profile height of profile curve for a roughness profile.
Figure 25 Surface Roughness Tester SJ-210, Type: SJ-210.
Figure 26 Example of a Map Showing Measurement Points on the Slab.
Figure 27 Example of Loaded Slabs Awaiting Cold Grinding.
Figure 28 Position of the Samples on the Slabs.
Figure 29 Cut Slab Samples.
Figure 30 Standardized Sample Pieces.
Figure 31 Hot Press Used During the Project.
Figure 32 Sample Pieces Correctly Centered in the Hot Press.
Figure 33 Powder Distributed Over the Sample Pieces in the Hot Press.
Figure 34 Fully Encapsulated Sample After Hot Pressing, Ready for Further Processing.
Figure 35 The cold and hot ground surface roughness for production slabs.
Figure 36 Ra and Rz surface roughness for production slabs.
Figure 37 Cast surface (non-ground slab).
Figure 38 Multiple Encapsulated Sample Pieces Mounted for Polishing and Further Processing.
Figure 39 Duplex 2205 cross section of oxide, at a location with thicker oxide, magnification 100X.
Figure 40 Oxide/casting powder mixture present in the bulk.

Figure 41 Example of oxide/casting powder layers on a Forta DX 2205 slab surface. Oxide/casting powder mixture < 25 µm thick (left image) and oxide/casting powder mixture ~ 200 µm thick (right image).
Figure 42 lement maps, 15kV EDS. Inner oxide layer is mainly enriched in Cr, outer layer is mainly enriched in Mn, Al, Mg and Ca. Na is more widely spread.
Figure 43 Cross section of Duplex 2205 slab surface at a section with a slightly thicker oxide/casting powder mixture (< 25 µm), see EDS analyzation results in Table 1 below. Thickness < 25 µm.
Figure 44 Oxide and casting powder mixture at Duplex 2205 slab surface, total thickness < 25 µm.
Figure 45 As in the maps, elements from casting powder (outer layer) and mainly Cr oxide (inner layer).
Figure 46 Oxide and casting powder mixture at Duplex 2205 slab surface.
Figure 47 Cross section of a thicker (~ 200 µm) oxide/casting powder mixture on the slab surface.
Figure 48 Cast surface (hot ground surface).
Figure 49 Cross section of a thicker (~ 200 µm) oxide/casting powder mixture on the slab surface.
Figure 50 Sample 2 surface, FEG-SEM image, SE detector 12 kV.
Figure 51 Sample 2 surface, FEG-SEM image, BS (back scatter) detector 12 kV.
Figure 52 Sample 2, EDS map, 12kV. Casting powder remaining on top of the slab surface.
Figure 53 Sample 2, backscatter detector, 12kV, EDS results are shown in Table 4 below.
Figure 54 Cold ground surface, 45°.
Figure 55 Sample 3 surface, FEG-SEM image, SE detector 12 kV.
Figure 56 Sample 3 surface, FEG-SEM image, BS (back scatter) detector 12 kV.
Figure 57 Sample 3, EDS map, 12kV.
Figure 58 Sample 3, backscatter detector, 12kV, EDS results are shown in Table 5 below.
Figure 59 Spectrum 19 (grey) and 20 (red). Note the slightly higher C peak in spectrum 20.
Figure 60 Grinding Wheel for Processing Slabs
Figure 61 Slab after cold grinding.
Figure 62 The Diagram Shows the Scrap Rate for the Three Different Methods.

List of Tables

Tabell 1 The chemical composition of duplex stainless steel 2205.
Tabell 2 Nominal Slab Dimensions in the Cold State.
Tabell 3 Nominal Slab Dimensions in the Cold State for Processed Slabs Used in the Project.
Tabell 4 Grinding Parameters Overview for Coarse and Fine Grinding.
Tabell 5 Grinding Parameters Overview for Coarse Grinding.
Tabell 6 Grinding Parameters Overview for Coarse Grinding.
Tabell 7 First Polishing Step Details.
Tabell 8 Second Polishing Step Details.
Tabell 9 Final Polishing Step Details.
Tabell 10 Test Results for Hot-Ground Slabs.
Tabell 11 Test Results for Cold-Ground Slabs.
Tabell 12 Test Results for Slab Set 543145 – 3.
Tabell 13 Test Results for Slab Set 543145 – 2.
Tabell 14 Test Results for Slab Set 543145 – 1.
Tabell 15 EDS analyzation results,15kV, normalized results (wt%).
Tabell 16 EDS analyzation results,15kV, normalized results (wt%).
Tabell 17 EDS analyzation results,15kV, normalized results (wt%).
Tabell 18 EDS analysis results, 12kV, normalized results.
Tabell 19 EDS analysis results, 12kV for shallow surface analysis. Normalized results, wt%.
Tabell 20 Comparison of Material Consumption Between Method 1 and Method 2.
Tabell 21 Comparison of Time Consumption Between Method 1 and Method 2.

1. Introduction

Outokumpu Avesta is an integrated facility where the entire production chain, from raw materials to finished products, is located on the same site and provides other Outokumpu units with material (slabs and coils) for further processing. The company converts recycled scrap into high-quality stainless steel. Outokumpu is a global leader in stainless steel production, specializing in steel thicknesses ranging from 1.5 mm to 12.7 mm. The company places a strong emphasis on sustainability and innovative technologies to meet future demands effectively. Outokumpu Avesta is also recognized for its two-meter-wide plates and coils, with a long-standing tradition of producing high-quality materials for various industries, including the automotive and construction sectors.

With increasing demands for efficiency, product quality, and environmental responsibility, Outokumpu continuously develops its processes to maintain competitiveness in the global market. This thesis focuses on a specific aspect of Outokumpu's production process: analyzing and improving the grinding process. By integrating theoretical insights with practical applications in the production environment, the work aims to support the company’s ongoing improvement initiatives and enhance overall productivity.

1.1 Background

Grinding slabs in Avesta has long been an essential step to deliver high-quality slabs that are subsequently converted into coils with minimal surface defects. In Avesta, there are four different processing routes a slab can take after casting:

Unground – Slabs rolled with the as-cast surface.
Hot-ground – Slabs ground transversely at high temperatures immediately after casting.
Cold-ground – Slabs ground longitudinally at temperatures below 100°C.
Hot-ground + Cold-ground – Slabs first hot-ground and subsequently cold-ground.

The selected processing route is, in most cases, predetermined but additional grinding, predominantly cold grinding, can be applied when necessary. The route chosen depends on the final product, the customer’s specifications, and the steel composition.

The choice of processing route is a critical factor for the product as it directly affects cost, lead time, and quality. Over the years, more steel grades have been introduced, and processes have evolved. However, continuous evaluation and potential changes to the processing route are rare, as deviating from the standard path carries economic risks. Research regarding the impact of grinding on the final product quality remains limited and is primarily based on internal studies.

1.2 Purpose

The aim of this study is to explore opportunities for cost reduction in production by optimizing surface treatment processes for DX 2205 Stainless Steel. The primary objective is to minimize grinding time and material consumption to reduce overall production costs. By analyzing and improving grinding processes—specifically through testing and adjusting various machine settings—the study seeks to enhance daily material processing efficiency. This optimization could lead to increased production volumes and improved profitability.

1.3 Research Questions

In the initial phase of the project, several key research questions were identified, which this report seeks to address:

- What surface quality is achieved with the current slab processing routes?
- Which methods are the most effective for preparing and analyzing slab samples efficiently?
- How do machine settings, such as pressure, speed, and stroke width, affect surface finish during cold grinding?
- Are there opportunities to reduce lead times and material consumption, particularly the use of grinding wheels, without compromising product quality?

1.4 Delimitations

This thesis focuses on the processing of Duplex 2205 stainless steel, (specifically examining oxidation levels following different grinding methods. The study includes three primary test scenarios:

1. Material processed through hot grinding – two passes: one coarse and one fine.
2. Material processed through a combination of cold and hot grinding – a total of four passes: two in hot grinding and two in cold grinding.
3. Material processed through a combination of cold and hot grinding – a total of three passes: two in hot grinding and one in cold grinding.

If time permits, a fourth test will be conducted on untreated material. Additionally, subject to available time, an analysis of potential savings in terms of time, material, and other resources will also be performed.

A key delimitation of this study is that only material sent to the Avesta cold rolling route (KBR) process will be examined. This restricts the processing and analysis to specific conditions and material types, excluding other potential variables that could influence the results.

1.5 Company

Outokumpu's history dates back to 1910 with the discovery of copper in Kuusjärvi, Finland, on a hill known as Outokumpu, which translates to “strange hill.” Over the decades, the company evolved from mining and refining various metals both domestically and internationally to focusing exclusively on stainless steel production in the 2000s [1].

A pivotal moment occurred in 2012 with the acquisition of Inoxum GmbH, which solidified Outokumpu's position as a global leader in stainless steel [1].

1.5.1 Historical Development of Avesta Works

Avesta Works has a history tracing back to the 14th century with iron processing at the Avesta rapids. In 1831, copper production ceased, and Avesta transitioned into a commercial steel mill. A major milestone occurred in 1905 when Axel Johnson acquired the facility. In 1924, the world’s first pure chromium steel was delivered from Avesta to England.

The 1930s saw growth with the construction of the first cold rolling mill and international orders. In 2001, the formation of Avesta Polarit AB through a strategic merger marked another development. In 2002, AvestaPolarit became a wholly owned subsidiary of Outokumpu [2].

1.5.2 Avesta’s Role within Outokumpu

The Avesta facility plays a pivotal role in Outokumpu’s operations, focusing on wide materials, including specialized grades within the Forta, Ultra, and Therma series. It supplies black hot-rolled coils to Nyby and Germany, as well as slabs to Degerfors for quarto plates.

Avesta Prefab specializes in components for suction roll shells and provides heavy plate processing services [2].

1.5.3 General Process Route

The following outlines the production pathway for stainless steel at Avesta Works:

1. Scrap: The raw material, comprising scrap and alloys, is delivered to the facility by train or truck from global suppliers.

2. Preheating: The scrap is loaded into a scrap basket and preheated to approximately 300°C. This critical step eliminates moisture, mitigating the risk of explosions during subsequent melting in the electric arc furnace.

3. Electric Arc Furnace: The scrap and alloys are melted in the electric arc furnace (EAF). The molten metal is then tapped into a ladle and transported to the converter for further processing.

4. AOD Converter: Within the converter, the carbon content of the steel is reduced, and additional alloys are introduced to achieve the required chemical composition.

5. Ladle Furnace: The ladle furnace is used for fine-tuning the steel's chemical composition while maintaining the correct temperature in preparation for the casting process.

6. Continuous Casting: The molten metal is cast into steel slabs of specified widths and thicknesses. These slabs are then cut to predetermined dimensions at a cutting station.

7. Hot Grinding: The surface quality of the slabs is improved through a hot grinding process.

8. Cold Grinding: An additional grinding process further refines the surface quality for selected materials.

9. Walking Beam Furnace: The slabs are reheated in a walking beam furnace to the appropriate temperature for the subsequent rolling stages.

10. Roughing Mill: At this stage, the slabs are rolled into long, thin sheets, referred to as "hot bands." These are then forwarded to the Steckel mill.

11. Steckel Mill: Equipped with two coiling furnaces, the Steckel mill rolls the sheets to the specified thickness before coiling them onto a mandrel.

12. Coiling: The rolled sheets are wound into coils, known as "black coils."

13. Annealing and Pickling (L-76): The coiled sheets undergo annealing in a furnace, followed by controlled cooling. Subsequently, the sheets are blasted, pickled, and thoroughly cleaned.

14. Inspection and Coiling: After a visual inspection to ensure quality, the coils are prepared for further processing.

15. Cold Rolling (Z-High): The cold rolling mill reduces the coil thickness according to customer specifications.

16. Finishing Line (L-2000): Thinner coils are cut into specified plate lengths and packaged. The line can also split coils into smaller rolls if needed.

17. Finishing Line (S-13): Thicker coils are cut into specified plate lengths and packaged for delivery.

18. Finishing Line (Slitter): This line is used for edge trimming or splitting the coils into narrower strips.

19. Terminal: The finished plates or coils are loaded onto trucks, rail cars, or containers for distribution to customers worldwide.

This process route highlights the precision and attention to detail applied at every stage of production, ensuring that the final stainless-steel products meet the highest quality and performance standards [2].

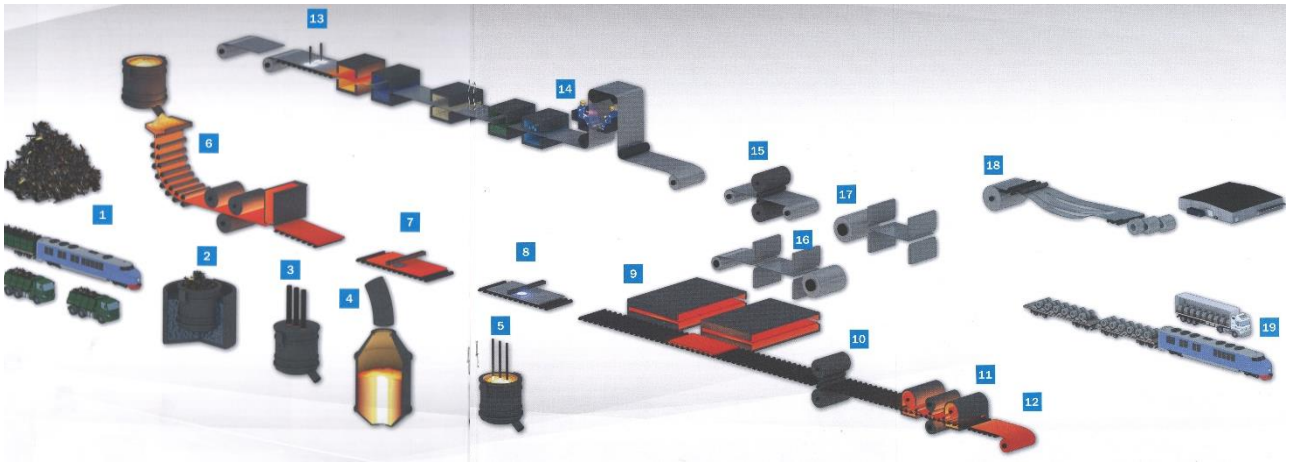

Figure 1: The Process Route at Outokumpu Avesta [2]

2. The Steel Grade in This Study

This chapter discuss the stainless steel groups in general and duplex grades in particular, with a focus on the 2205 Duplex stainless steel grade. This grade is the focus of this study.

2.1 Stainless Steel Groups in General

Stainless steel can be categorized into five primary groups, each characterized by distinct properties and specific areas of application.

Austenitic stainless steel is the most widely used group, valued for its exceptional corrosion resistance. This makes it particularly suitable for applications such as sinks, pipes, and other components exposed to corrosive environments. Austenitic stainless steel contains high levels of chromium (Cr) and nickel (Ni), a low carbon content (C), and often includes molybdenum (Mo) as an alloying element to enhance its resistance to pitting and crevice corrosion. Figure 2 shows a typical austenitic microstructure.

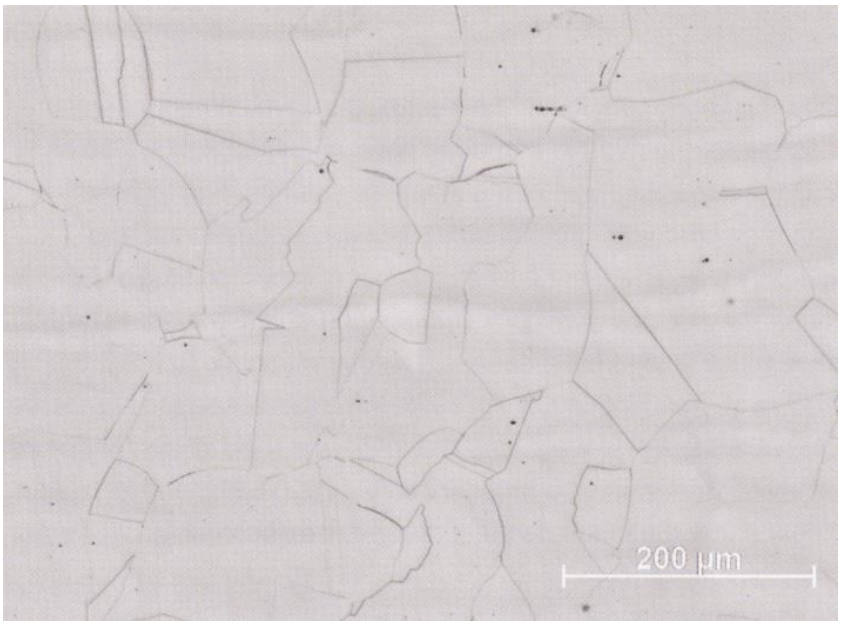

Figure 2: Austenitic microstructure.

Martensitic stainless steel is notable for its ability to be hardened, making it well-suited for applications requiring high strength and wear resistance, such as cutting tools, knives, and surgical instruments. This type of steel typically contains a high carbon content (C), a low amount of chromium (Cr), and minimal to no nickel (Ni). These properties enable martensitic steel to undergo hardening processes, enhancing its durability and performance in demanding applications. Figure 3 shows a typical martensitic microstructure.

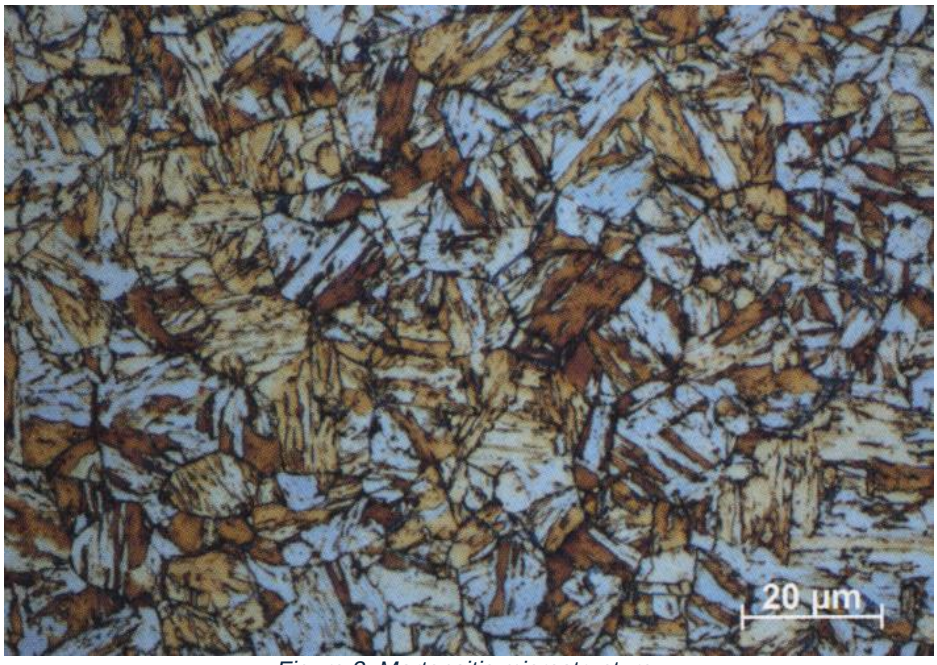

Figure 3: Martensitic microstructure.

Ferritic steel is characterized by its high chromium content and low nickel content, making it a cost-effective option for various applications. Due to its excellent corrosion resistance and affordability, ferritic steel is commonly used in products such as refrigerator doors and handles. Figure 4 shows a typical ferritic microstructure.

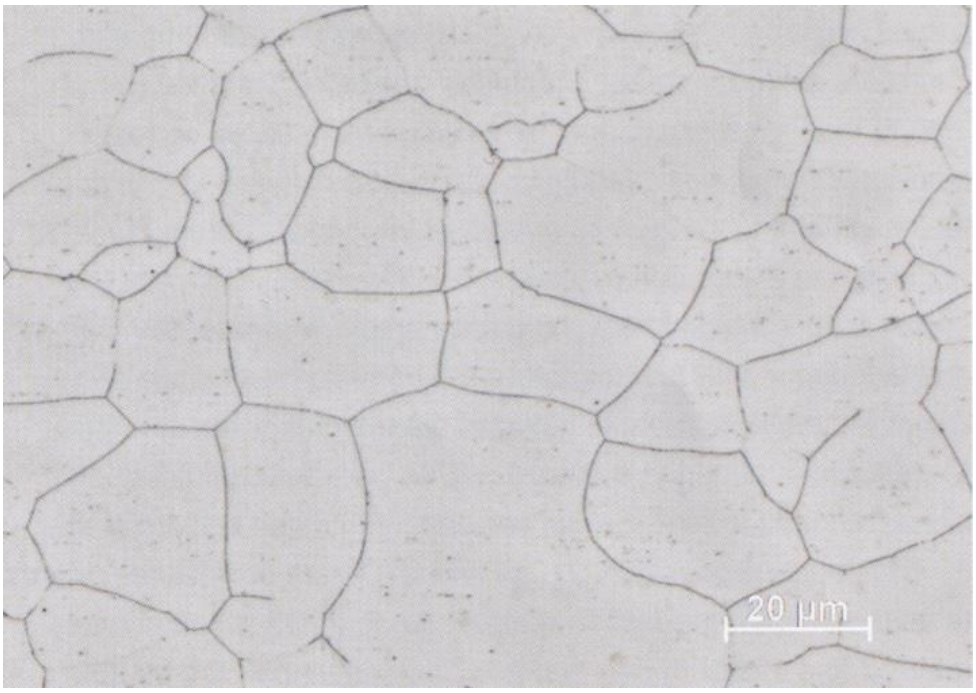

Figure 4: Ferritic microstructure.

Duplex steel combines the strength and corrosion resistance of both ferritic and austenitic steel, making it suitable for use in bridges and pressure vessels. It typically consists of 55% ferrite and 45% austenite. The steel has a high chromium (Cr)

content, medium nickel (Ni) content, low carbon (C) content, and often includes a small amount of molybdenum (Mo). Figure 5 shows a typical duplex microstructure. [3][8]

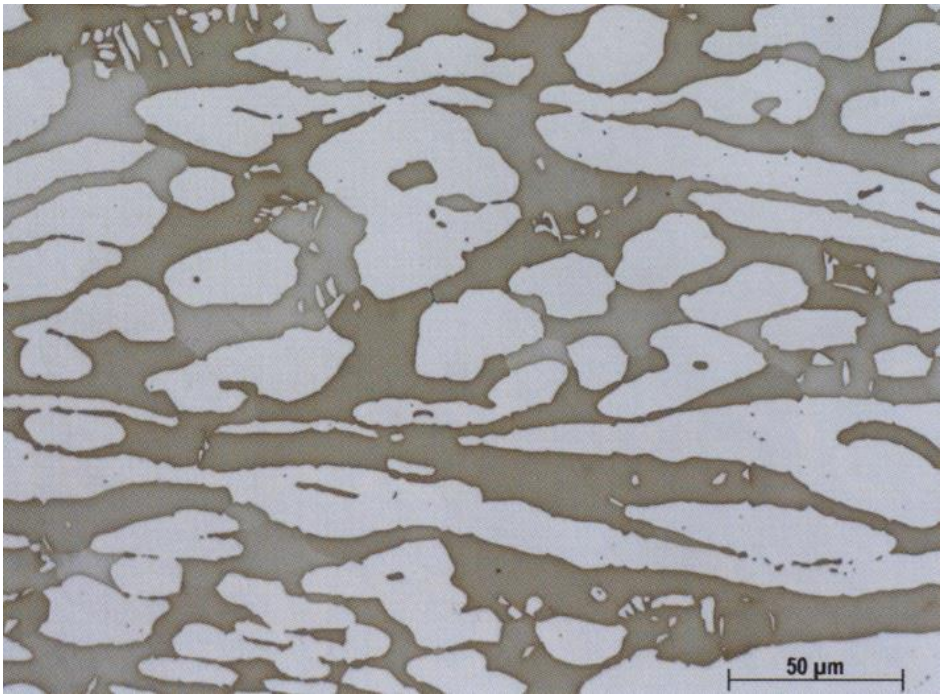

Figure 5: Duplex microstructure.

Precipitation-hardened (PH) steel is recognized for its high strength and durability, making it suitable for specialized applications such as golf clubs. This type of steel typically contains 15–17% chromium (Cr), 4–8% nickel (Ni), a low molybdenum (Mo) content, and up to 5% copper (Cu) [8].

2.2 What is Duplex Stainless Steel?

Duplex stainless steels are distinguished by their unique microstructure, which consists of approximately equal proportions of ferritic and austenitic phases (typically 50% ferrite and 50% austenite). This two-phase structure enables duplex stainless steels to combine the advantageous properties of both ferritic and austenitic stainless steels. Specifically, duplex steels offer high mechanical strength, superior corrosion resistance—particularly against stress corrosion cracking—and good toughness, making them well-suited for demanding applications across various industries [3].

The exceptional strength of duplex stainless steels is primarily achieved through the addition of nitrogen as an alloying element. In addition, these steels demonstrate excellent resistance to wear and erosion, high energy absorption, and low thermal expansion, which further enhances their performance in challenging environments.

Due to their combination of strength, durability, and corrosion resistance, duplex stainless steels are widely employed in industrial sectors such as the chemical industry, food processing, pharmaceuticals, and marine applications. Their ability to maintain mechanical integrity and ensure a long service life makes them an ideal choice for applications where both reliability and performance are critical requirements [3].

The development of duplex stainless steels represents a relatively recent innovation, with the first alloys introduced in the 1950s. As illustrated in the diagram, the timeline from the 1970s highlights a clear distinction between the first and second generations of duplex stainless steels.

The early first-generation alloys were notably challenging to weld, which significantly restricted their applicability across various industries. In contrast, second-generation alloys were specifically developed to address this limitation, offering improved weldability and expanding their use in a wider range of applications.

2.3 Duplex 2205 Stainless steel

Duplex 2205 is a two-phase steel grade within the duplex stainless-steel category, known for its high yield strength, which is approximately twice that of standard austenitic stainless steels. In addition to its superior mechanical properties, Duplex 2205 demonstrates excellent fatigue strength and outstanding resistance to various forms of corrosion, including stress corrosion cracking, pitting, erosion, and general corrosion, particularly in demanding and aggressive environments [3].

2.3.1 Chemical Properties

The typical chemical composition of Duplex 2205 is shown in Table 1.

Table 1: The Chemical Composition of Duplex Stainless Steel 2205. [6]

Steel name	UNS	C	N	Cr	Ni	Mo
2205	S32205	0.02	0.17	22	5.7	3.1

2.3.2 Corrosion Resistance

Duplex 2205 is a high-performance stainless steel renowned for its exceptional corrosion resistance, which is primarily attributed to its elevated levels of chromium, molybdenum, and nitrogen. These alloying elements play a crucial role in preventing pitting and crevice corrosion, even in challenging environments involving both oxidizing and acidic conditions.

The combination of high chromium and molybdenum content, along with the addition of nitrogen, significantly enhances the material's ability to resist chloride-induced stress corrosion cracking. This makes Duplex 2205 particularly well-suited for applications in marine environments and other highly corrosive settings.

Duplex 2205 maintains its corrosion-resistant properties at temperatures up to approximately 150°C thereby broadening its range of industrial applications. Additionally, the ferritic phase within its microstructure provides good resistance to strongly alkaline environments, further increasing the material's versatility across a wide range of industries [5].

2.3.3 Heat Resistance

Like other duplex stainless steels, Duplex 2205 demonstrates good resistance to oxidation at elevated temperatures, enabling its use in applications where high-temperature exposure is a factor without a rapid loss of its protective properties.

However, Duplex 2205 is susceptible to embrittlement when exposed to temperatures above 300°C for prolonged periods. This embrittlement is caused by microstructural changes, such as the formation of the sigma phase, which can significantly compromise the material's mechanical properties.

To ensure long-term strength and performance, it is recommended that Duplex 2205 not be used at temperatures exceeding 300°C [5].

2.3.4 Heat Treatment

For Duplex 2205, an annealing temperature in the range of 1020 to 1100°C is recommended to restore the material’s microstructure following welding or other thermal exposures. Unlike conventional steels, Duplex 2205 cannot be hardened through traditional heat treatment methods, such as quenching and tempering. However, the material can be strengthened through mechanical processing, as it demonstrates the ability to harden during cold working.

During heat treatment, it is essential to account for the material’s relatively high thermal expansion coefficient to minimize the risk of warping or deformation, particularly in larger components [5].

2.3.5 Machining – Mechanical Processing

Machining Duplex 2205 presents greater challenges compared to austenitic stainless steels in the 300 series, primarily due to its higher strength and hardness. These properties require greater cutting forces and result in faster tool wear, which can negatively impact productivity.

To achieve optimal results, the use of powerful and rigid machines with robust clamping of both the tools and workpieces is strongly recommended. Minimizing vibrations is crucial and can be achieved by ensuring the tool overhang is kept as short as possible [5].

3 Grinding

3.1 The Origin and Development of Grinding

Grinding is a material removal process with a history spanning over two millennia, tracing its origins to ancient times. Historically, grinding served primarily as a finishing method for products such as knives, tools, and weapons. Beyond sharpening blades, grinding also played a significant role in construction, particularly in the processing of stones for monumental architecture, such as the pyramids.

With the onset of the Industrial Revolution, grinding became increasingly essential in modern technologies, where the abrasive industry emerged as a cornerstone of various manufacturing processes. This shift was driven by the rising demand for the complex geometries required in contemporary machinery.

By the 19th century, grinding had further evolved as a critical metalworking process. Its role in the production and refinement of hardened steel established it as an integral process, where it remains indispensable to this day [10].

3.2 What is Grinding?

Grinding is a cutting process where the cutting edges are formed by abrasive grains. It is considered one of the advanced manufacturing processes and involves the use of high-speed abrasive wheels as cutting tools. Grinding is commonly used in metalworking and is recognized for its ability to produce high-quality and fine surface finishes.

The grinding process involves a rotating grinding wheel and consists of two main components: abrasives and bonding agents. The abrasives are particles that act as cutting tools, while the bonding agent holds the abrasive grains together and provides the wheel with its structure and shape.

The purpose of grinding is to achieve a flat, cylindrical, or conical surface on the material. Key components in a grinding operation include the grinding machine and the workpiece, which are essential to the process.

The grinding wheel functions by removing a layer of material as it moves across the workpiece. This layer typically consists of unwanted material that is removed to shape and adapt the workpiece to the required dimensions and specifications as defined by the customer [10][11].

3.3 Composition of grinding tool

The composition of the grinding tool refers to the combination of abrasives, grain size, bonding agents, and hardness grade. This composition is carefully selected, as varying it allows for modifying the properties of the grinding wheel to suit different grinding operations [13][16].

Abrasives consist of abrasive particles that act as cutting tools to perform the grinding process. The most commonly used abrasives in grinding wheels include aluminum oxide (Al_2O_3), silicon carbide (SiC), CBN (cubic boron nitride), and diamond [10][11].

Bonding agents hold the abrasive grains together and provide the grinding wheel with its structure and shape. The three most common types of bonding agents are ceramic bonds, phenolic resin bonds, and rubber bonds [16].

Pores (Porosity) consist of small voids within the grinding wheel and serve as spaces for the transportation of coolant, heat dissipation, and chip formation during grinding. The purpose of pores is to reduce the risk of overheating during the process [13]. See Figure 7 for an illustration of the structure of the grinding wheel.

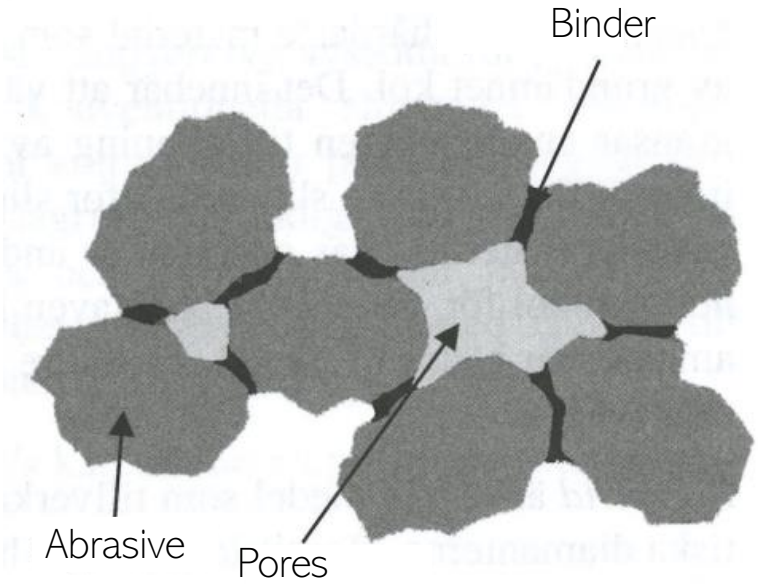

Figure 7: Structure of the Grinding Wheel [13].

3.4 Grinding Methods

Grinding is a central machining process with several distinct methods. The choice of grinding method depends on the specific material to be processed, the desired surface finish, and the precision requirements. While there are numerous grinding methods, the most significant ones include:

- Cylindrical grinding
- Surface grinding
- Internal grinding
- Centerless grinding
- Fine and rough grinding

Surface grinding is an essential grinding method used for machining flat surfaces. The method operates by rotating the grinding wheel over the surface of the workpiece, which is clamped onto a worktable that moves back and forth in a linear motion. This method is commonly applied in manufacturing processes where flat surfaces are required, such as slab grinding at Avesta Works. See Figure 9 [13].

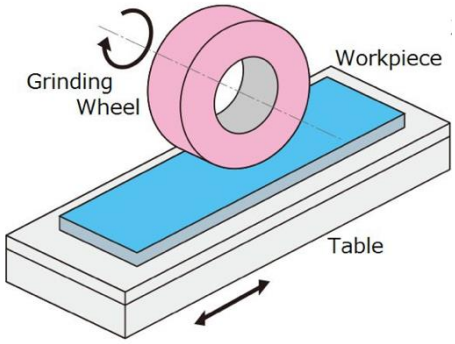

Figure 8: Surface grinding. [15]

When it comes to rough and fine grinding, these are two distinct grinding methods. Rough grinding is a faster process that uses higher pressure to remove large amounts of material efficiently, with the primary goal of quickly shaping the workpiece. In contrast, fine grinding is a method that operates at lower pressure than rough grinding, providing greater precision and is primarily used to achieve a smooth surface finish.

3.5 Work Materials

The efficiency and results of the grinding process depend on the choice of work material. The most common materials for grinding in the industry are cast iron and steel, which, due to their specific properties, place different requirements on both tools and techniques.

Cast Iron:
Cast iron contains flake-shaped graphite, which acts as a lubricant and facilitates chip breaking, making the material highly machinable. The same type of grinding wheel suitable for cast iron can also be used for malleable iron and ductile iron, as these materials share similar properties to steel.

Toughened and Untoughened Steel:
These materials are typically processed using abrasives containing aluminum oxide, a material known for its durability and toughness. Aluminum oxide is primarily used for grinding applications requiring a wear-resistant and robust abrasive that can effectively handle the specific properties of steel without compromising the grinding results.

Hardened Steel:
Hardened steel often demands a more brittle and harder abrasive to enable the grinding wheel to cut efficiently into the material.

High-Alloy Steel:
High-alloy steels, such as high-speed steel, can be particularly difficult and challenging to grind due to their high content of hard carbides and a resistant base material. These characteristics result in increased grinding resistance, requiring customized abrasives and techniques to achieve efficient results.

Stainless Steel:

Ferritic-austenitic stainless steels, such as Duplex 2205, as well as austenitic and ferritic grades, are typically ground using abrasives characterized by sharp-edged grains. While grinding these materials produces optimal results, the process incurs higher costs compared to more common steel grades. This is due to stainless steel's specific properties, such as its tendency to work-harden, low thermal conductivity, and toughness, which demand adapted abrasives and grinding techniques [13].

3.6 Contact Geometry

A critical factor in machining processes is the cutting interface, as it provides a clear understanding and defines the contact situation between the workpiece and the tool, see figure 9. At Outokumpu Avesta Works, specifically in the cold grinding process, surface grinding is used to produce a flat surface on the material. This machining process is considered one of the simplest grinding operations. The process operates as follows: a grinding wheel with a diameter d_s rotates at a peripheral speed v_s, while a material depth a_e is removed from the workpiece. The material depth a_e is simultaneously machined as the workpiece moves at a speed v_w [10].

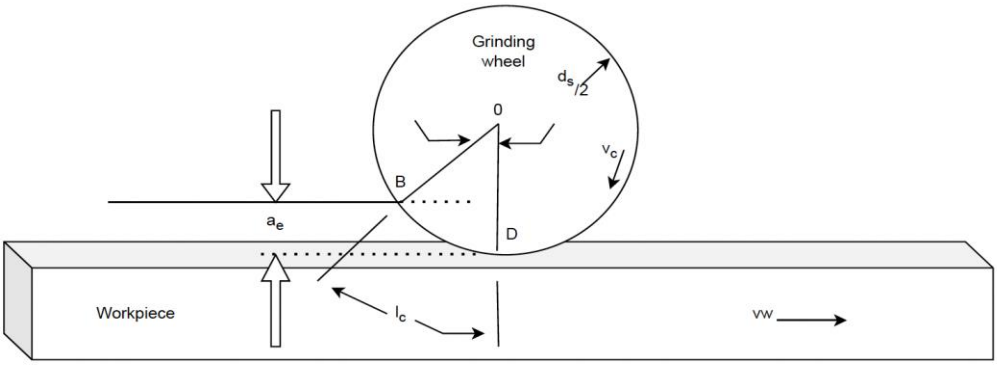

Figure 9: The Relationship Between the Workpiece and the Grinding Wheel in Surface Grinding.

When the grinding wheel penetrates the material during the grinding process, a contact arc is formed where the actual grinding occurs. As shown in Figure 13, the length of the contact arc between the grinding wheel and the workpiece is referred to as l_c. The value of l_c can be determined under the assumption that no relative motion or deformation occurs between the workpiece and the wheel during grinding. [10]

$$l_c = (a_e \times d_s)^{1/2} \quad (2)$$

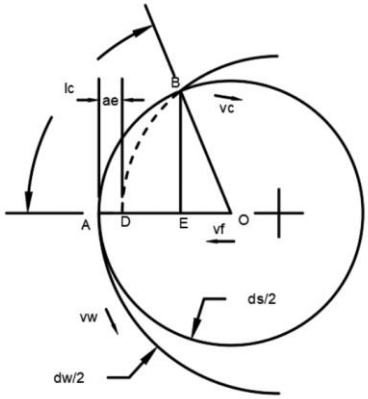

Figure 10: Internal Grinding of Cylindrical Components.

3.7 Grinding Forces:

Specific forces refer to the grinding forces acting on individual abrasive grains. The average specific force is obtained by dividing the total force, generated at the interface between the grinding wheel and the workpiece, by the number of active cutting grains. The number of grains can vary significantly as it depends on the size of the contact area and the cutting-edge density of the grinding path. The specific forces that arise are a determining factor in the work hardening of the material. See Figure 11 for an illustration of the grinding forces.

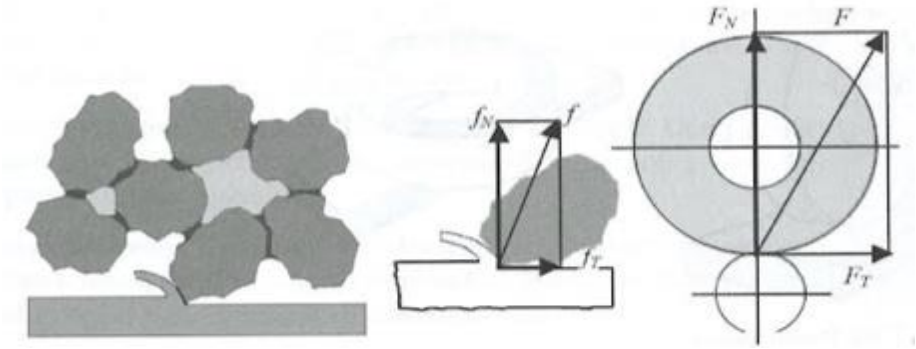

Figure 11: Grinding Forces [13].

The total force generated during grinding can be divided into a normal force and a tangential force. The tangential force (F_T) is the force that loads the grinding motor and determines power consumption. Since the tangential force is responsible for generating heat during the machining process, it is considered the frictional component of the normal grinding force. After several passes, the surface of the grinding wheel becomes duller, which can lead to an increase in the contact area. This, in turn, requires a significantly higher normal force (F_N) to achieve the same cutting depth as before [13].

An increase in the normal force (F_N) has consequences, including higher frictional losses, even though the coefficient of friction decreases due to the smoother contact area between the wheel and the workpiece [13].

3.8 Aggressiveness in Cold Grinding Processes:

In cold grinding processes at Outokumpu, aggressiveness refers to how effectively and quickly material is removed based on the applied force and chosen process settings. It indicates the intensity of the grinding process, which affects both productivity and surface quality.

High aggressiveness results in faster material removal, improving throughput. However, this can lead to a rougher surface, such as in hot-ground or unground materials. It also generates more heat and increases the risk of thermal damage. On the other hand, low aggressiveness provides a smoother surface finish and reduces thermal risks but slows down the process.[31][32]

Controlling aggressiveness is essential in cold grinding because it helps maintain the material's integrity and ensures a smooth surface. This is especially important in stainless steel production, where even minor surface defects can affect performance.

Key factors that influence aggressiveness include:

Cutting speed (V_c): Higher speeds increase material removal but may generate more heat.

Feed rate (V_f): Faster feed rates speed up processing but can reduce surface quality.

Depth of cut (ap): Deeper cuts remove more material but raise the risk of damage.

Grinding wheel structure and grain size: Coarser grains remove material faster but may harm surface quality, while finer grains provide a better finish but slow the process.

These parameters will be discussed in more detail later in the report, highlighting how Outokumpu can achieve a balance between efficient material removal and the high surface quality required for stainless steel products.

4 Grinding Production

4.1 Grinding Process

To understand the grinding mechanism, it is essential to analyze how the grinding process is implemented in a grinding machine and the angle at which the grinding wheel operates during the process. The grinding process, also referred to as material removal through grinding, is an industrial manufacturing process in which a grinding wheel is used to remove material from slabs.

The grinding process can be divided into several stages, with the two primary grinding methods being fine grinding and rough grinding. The grinding wheel can operate at two main angles $90°$and $45°$. [17]

The $90°$ grinding angle, see figure 15, is most commonly used for surface finishing and edge processing to achieve optimal surface quality. When grinding at a $90°$ angle, the grinding wheel experiences more uniform wear, leading to an extended service life [12].

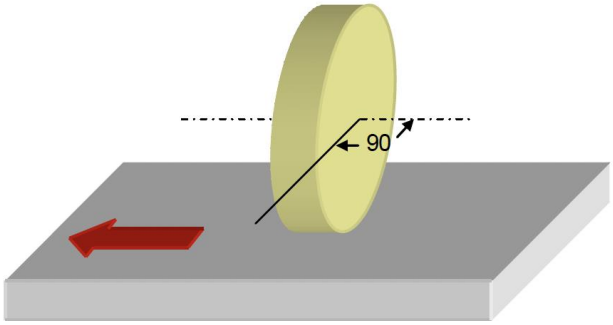

Figure 12: $90°$ set up angle.

The $45°$ grinding angle, see figure 16, is primarily used for rough machining, which in turn results in higher productivity. However, the disadvantage of using a $45°$ angle is that it leads to faster wear and an uneven surface on the grinding wheel, which subsequently results in reduced surface quality [12].

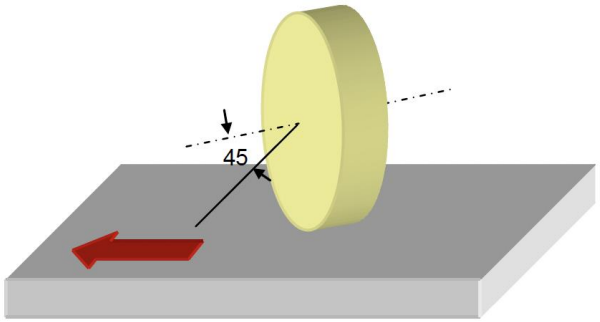

Figure 13: $45°$ set up angle.

Rough grinding is a grinding process used to remove large amounts of material with the primary objective of quickly shaping the workpiece. It is also employed to eliminate oxide layers formed during casting, as well as defects or excess material. As a result, rough grinding does not achieve high surface finish or tight tolerances.

Fine grinding is another grinding process, primarily used to improve surface finish and shape the workpiece. This is typically accomplished by reducing the cutting depth, in contrast to rough grinding, which operates with a greater cutting depth.

4.2 The Material Removal Process

Grinding of slabs is an advanced and complex material removal operation that involves cutting, rubbing, and plowing, depending on the interaction between the abrasive grains and the work material during the grinding process. The process is considered probabilistic, as a large number of abrasive grains with varying and often unknown geometries changing over time remove material and influence the process [10][20].

The process operates such that a grinding wheel begins cutting the slab (material) as the workpiece pass underneath it, see Figure 14. This interaction generates tangential and normal forces between the grinding wheel and the workpiece. These forces enable the abrasive grains of the grinding wheel to penetrate into the surface of the slab [10].

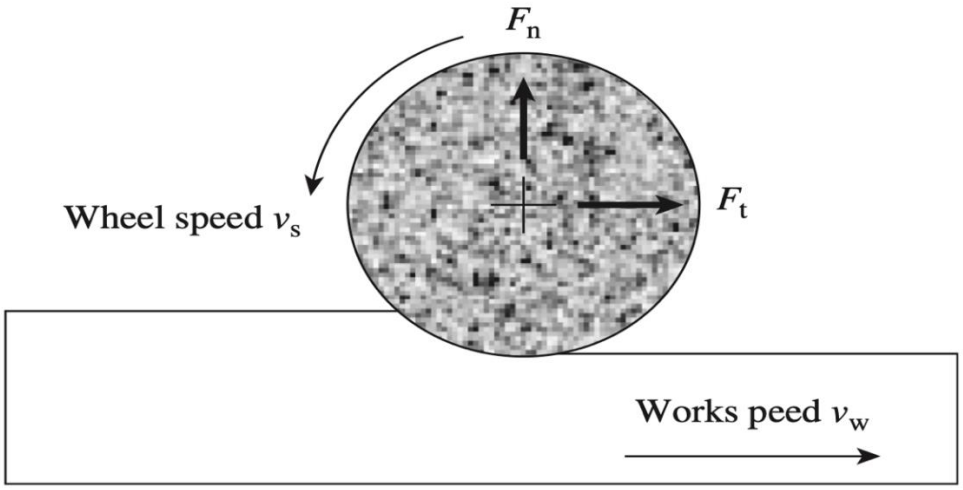

Figure 14: Material removal process. [10]

During the material removal process, abrasive grains penetrate deeply into the material. Some of the abrasive grains cut deeply into the slab, producing chips, while others on the grinding wheel only interact with the surface, causing minimal penetration. These minimally penetrating grains result in light abrasion and surface deformation of the slab [10][21].

Plowing occurs when the grains penetrate the slab's surface without immediately removing material or creating chips [10][21]. See Figure 15 for an overview of the described parameters.

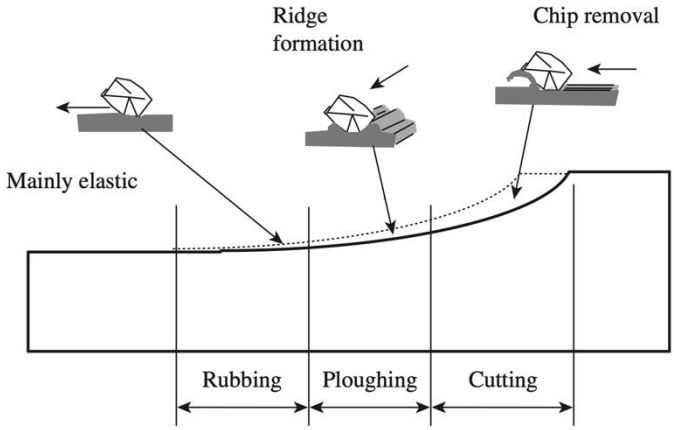

Figure15: Ploughing rubbing and cutting occur as grain penetration progressively increases within the constant arc. [10]

Cutting, rubbing, and plowing are the three primary stages that occur during the grinding process of slabs. These stages are common to all materials. However, the extent to which each stage occurs is influenced by the material's physical properties, its reactivity to the abrasive, the surrounding environment, and its deformation characteristics [21].

Several key parameters emerge during grinding, which can significantly impact the process. One critical aspect is the depth of grain penetration, which can be influenced by the grinding wheel's rotational speed, the feed rate of the workpiece, and the grinding depth. These parameters are manually controlled during the grinding process. Variations or inaccuracies in these inputs can affect grinding forces, significantly increase energy consumption, and impact surface finish and wheel wear [20].

Determining the exact depth of grain penetration can be challenging; however, the effects can be altered and improved by adjusting grinding parameters. For example, modifications to speed, feed rate, and grinding depth can enhance the efficiency of the grinding process.

4.3 Grinding process routes at Avesta Works

The three different process routes currently applied at Outokumpu Avesta Works are cold grinding, hot grinding, or no grinding at all (cast surface). The choice of process route largely depends on several key factors, including desired surface quality, economic considerations, and product properties.

Figure 16: 90° grinding in progress.

When it comes to surface quality and aesthetic requirements, cold grinding ranks highest. Cold grinding is often used to enhance the surface finish of steel products requiring high aesthetic quality, such as kitchen appliances. In cold grinding, the surface is refined after cold rolling, removing defects and improving appearance. In contrast, hot grinding is employed to remove surface defects formed during hot rolling, typically for slabs intended for products that do not require as fine a surface finish as kitchen equipment [18][19].

In certain specific cases, such as hot-rolled products processed at high temperatures, hot grinding is often necessary to remove surface layers, whereas cold-rolled products may require cold grinding to achieve a smoother surface finish. However, in cases where products meet quality standards at earlier production stages, grinding can be omitted [18][19].

Grinding processes, regardless of the chosen process route, generally lead to increased manufacturing costs. Thus, it is often more cost-effective to skip grinding if the final product already meets customer expectations. The goal is to minimize grinding, as it results in a material loss of 2–3%. Additionally, the need for cold grinding increases lead times, which is an important factor to consider in production planning.

4.4 Cold grinding process routes at Avesta Works

This section illustrates the general path when cold grinding a slab. Figures 21 to 24 shows the process steps, showing both 45° and 90° grinding.

Figure 17: Hot ground slabs ready for cold grinding

Figure 18: 90° grinding in process

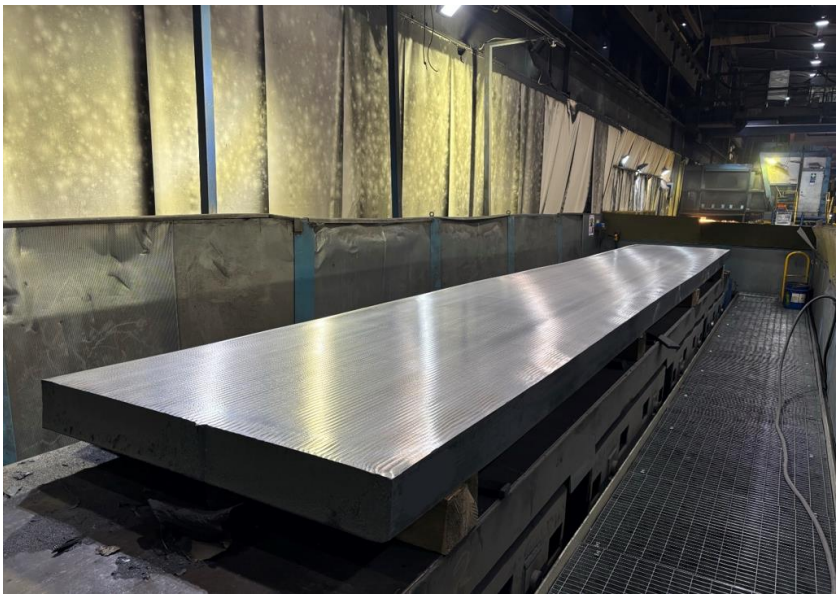

Figure 19: Slab after cold grinding

Figure 20: Used grinding wheels

5 Surface Roughness and Its Parameters

5.1 Roughness and its importance:

During the manufacturing process, microscopic surface irregularities can form as a result of mechanical machining processes, such as grinding. Surface roughness is an important metric used to describe surface quality by measuring the complex topography of the surface after machining. This topography consists of a series of peaks and valleys with varying heights over a small area of the material [23].

In physical systems and engineering, surface roughness has historically been regarded as a secondary effect, yet it plays a critical role in many technical disciplines, such as production engineering, aerospace, and road construction. Research has demonstrated that surface roughness has a significant impact and that its importance in technical applications should not be underestimated [22].

The increasing complexity and precision required in modern systems and industries have made the understanding and control of surface roughness essential for future advancements in engineering and technology. In industrial applications, this secondary effect has proven to be a critical factor in determining surface quality. Accurate measurement of surface roughness can influence key aspects such as friction and the interaction of surfaces with other components, for example, in bonding and sealing applications [22].

5.2 Workpiece surface measurement

The surface structure created on a workpiece can be defined by three key parameters: the Primary Profile (P-profile), the Roughness Profile (R-profile), and the Waviness Profile (W-profile). To calculate the Roughness Profile (R-profile), a cutoff filter must be applied to eliminate long-wavelength components from the Primary Profile (P-profile). This process results in the Roughness Profile (R-profile) being a controlled modification of the Primary Profile (P-profile) [28].

5.2.1 Basis for evaluation

When measuring the surface structure of a workpiece, the evaluation is typically based on a defined reference length. If a reference length is not specified in the design drawing of the component, the operator performing the measurement must determine the reference length independently.

There are three distinct measurement lengths: l_t, l_n och l_r. There l_t is the total length, which includes the start segment, evaluation segment, and stop segment. l_n is the evaluation length, which usually comprises five individual reference lengths. l_r The reference length, which defines the primary segment for evaluation [28], see Figure 21.

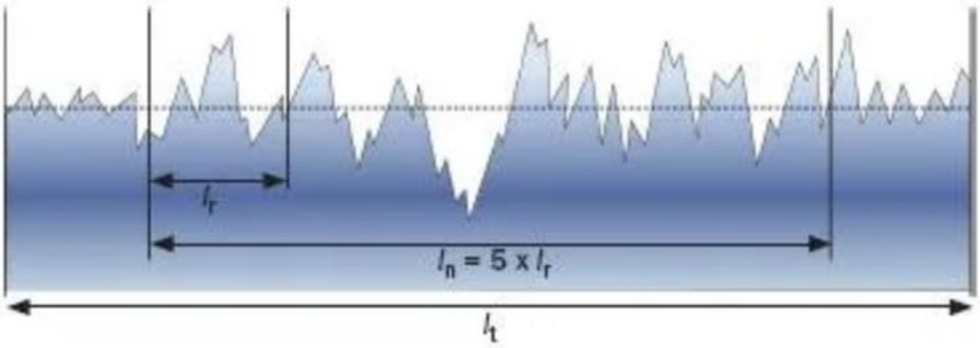

Figure 21: Measuring lengths. [28]

5.2.2 Arithmetic Mean Roughness (R_a)

R_a is the most commonly used parameter to describe surface roughness. It represents the arithmetic mean of the material surface profile deviations around a mean line and is relatively insensitive to extreme peaks and valleys, see Figure 26 [24][25].

$$R_a = \frac{1}{lr}\int_0^{lr} |Z(x)|dx \tag{9}$$

The lower the R_a value, the smoother the surface. For example, $R_a = 0{,}02\ \mu\text{m} \implies$ corresponds to a mirror-like finish. For metals, it is common for the $R_a -$ value to range between $0{,}02\ \mu\text{m}$ and $3{,}5\ \mu\text{m}$. [28]

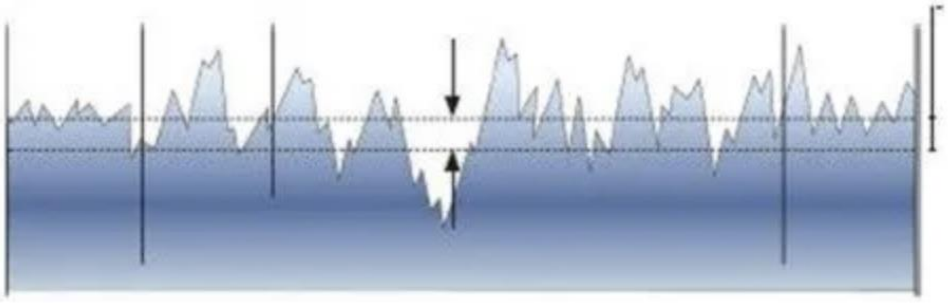

Figure 22: Arithmetical mean height for a roughness profile. [28]

5.2.3 Maximum Roughness Profile Height (R_z)

R_z represents the sum of the roughness profile's vertical distance between the maximum profile height $R_{z\,max}$ and the maximum profile depth $R_{z\,min}$ across the sampling length lr. R_z is calculated as the average of five reference lengths, although the number of reference lengths may vary depending on the measurement equipment, corresponding to the peak-to-valley distances [26]. See Figure 23.

$$R_z = R_{z\,max} + R_{z\,min} \tag{10}$$

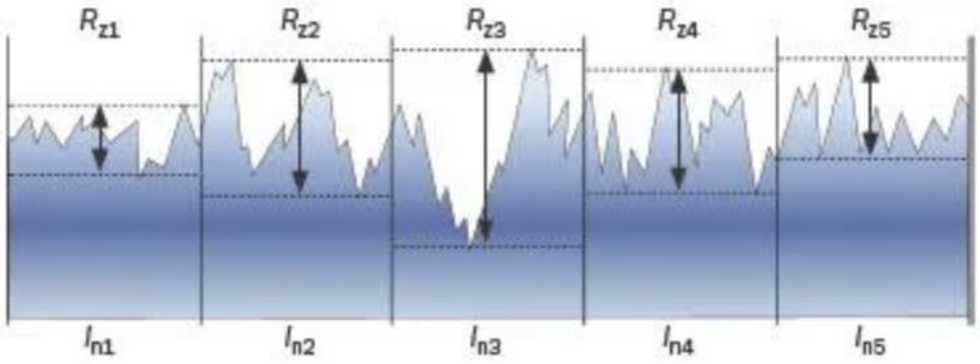

Figure 23: Maximum height of profile curve for a roughness profile. [28]

5.2.4 Total profile height (R_t)

R_t describes the total roughness of a surface within a measurement length by calculating the total height between the maximum profile peak and the maximum profile valley depth. This is typically based on five different reference values across the entire measurement length. R_t measures the maximum vertical deviation over a small area of the workpiece. This vertical deviation is interpreted as an indication of how uneven or rough a surface may be within a specified area [27]. See figure 24.

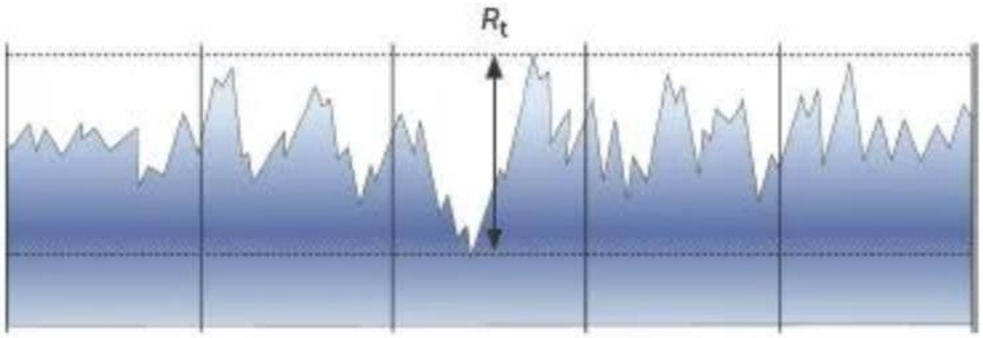

Figure 24: Total profile height of profile curve for a roughness profile.[28]

6 Methods

To develop a solution that functions effectively in practice, it is essential first to document the initial process thoroughly. Subsequently, a theoretical description of the process structure can be created, forming the basis for the final result. To ensure the functionality of the theoretical prototype, testing is conducted.

This section outlines the methodologies employed, including the preparation of test samples, grinding, analysis using Light Optical Microscopy (LOM) and Scanning Electrode Microscopy (SEM), and surface roughness measurements. The tests are designed to address the project's research questions.

6.1 Slab Dimensions

The slabs produced at Outokumpu Avesta have the following nominal dimensions presented in Table 2:

Table 2: Nominal Slab Dimensions in the Cold State.

Thickness	140 – 200 mm
Width	Typically ranges between 1150 and 2100 mm.
Length Range	3250 – 10950 mm.
Maximum Weight per Slab	25 000 kg.

Three slabs from the same melt (heat) were selected for testing. This ensures they have the same chemical composition and were manufactured under identical conditions, making them directly comparable. The dimensions used for all slabs in the project were predetermined and consistent across all slabs.
The dimensions for these slabs are presented in Table 3, which shows the size and weight of the material used throughout the project prior to processing. The **Sample ID** refers to the number assigned to each slab for the different grinding methods that are to be tested in this work

Table 3: Nominal Slab Dimensions in the Cold State for Processed Slabs Used in the Project.

	Sample 1	**Sample 2**	**Sample 3**
Weight In	24 870 kg	24 800 kg	24 890 kg
Length	10 220 mm	10 210 mm	10 205 mm
Width	1590 mm	1590 mm	1590 mm

6.2 Grinding Tests

In this experiment, three different slabs were tested on the same machine but under varying grinding conditions for each slab. All materials were processed using the CM3 grinding machine in the cold grinding facility to ensure consistent testing conditions. However, each slab underwent individual grinding processes, with parameters such as speed, pressure, and stroke width adjusted to evaluate their effects on surface quality and material removal. The parameters used for each method is presented in Table 4 to Table 6.
The surfaces after grinding with the different methods was investigated to ensure that no visible defects were seen, it is important that the surface remains free from defects after the grinding.

6.2.1 Method 1: Standard grinding process:

The slab named **Sample 1** was ground using standard grinding speed, pressure, and stroke width to evaluate how these parameters influence surface roughness and material removal. The slab was processed using the method that Outokumpu has employed for several years, referred to as code **60** grinding codes. This process includes two transitions, see Table 4.

Table 4: Grinding Parameters Overview for Coarse and Fine Grinding.

	Power	stroke width	table speed	grinding angle
Coarse grinding	110 kW	10 mm	80% (100% = 65 m/min)	45°
Fine grinding	60 kW	14 mm	80% (100% = 65 m/min)	45°

(power): Pressure setting in the control unit at Avesta (measured as power consumption)*

6.2.2 Method 2: Coarse grinding process:

The slab named **Sample 2** was processed using the same speed as Method 1 but with moderate pressure to compare results with those of Slab 1 and provide insights into how moderate grinding parameters affect the material. The slab underwent one pass on each side, see Table 5

Table 5: Grinding Parameters Overview for Coarse Grinding

	Power	stroke width	table speed	grinding angle
Coarse grinding	110 kW	10 mm (8 mm on edges)	80% (100% = 65 m/min)	45°

(power): Pressure setting in the control unit at Avesta (measured as power consumption)*

6.2.3 Method 3: Lower pressure grinding:

The slab named **Sample 3** was ground at low speed, low pressure, and a wider stroke to explore the effects on surface quality and to further develop the concept into a practical solution. The slab underwent one pass on each side, see Table 6.

Table 6: Grinding Parameters Overview for Coarse Grinding.

	Power	stroke width	table speed	grinding angle
Coarse grinding	100 kW	14 mm	50% (100% = 65 m/min)	45°

(power): Pressure setting in the control unit at Avesta (measured as power consumption)*

6.2.4 Surface Roughness Measurement Method

After each grinding operation, the surface quality was analyzed using a Mitutoyo SJ-210, see Figure 25 to evaluate the effects of the different grinding parameters. Prior to measurement, the instrument was calibrated using a standard reference (178-601) to ensure that the measurement results were as accurate and reliable as possible. The calibration was performed according to the manufacturer's specifications.

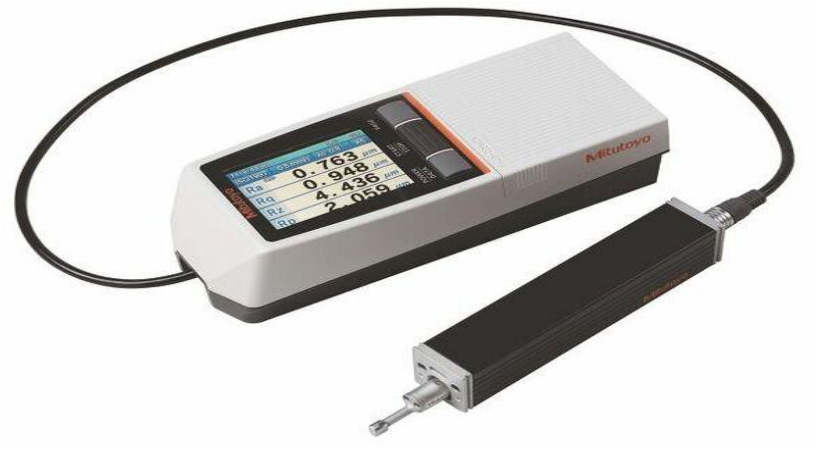

Figure 25: Surface Roughness Tester SJ-210, Type: SJ-210 [31].

The surface roughness measurements were conducted on five distinct areas, each measuring 10 mm x 10 mm, on each side of the slab. Measurements were taken at five selected points within this area to ensure the results were representative of the entire slab surface. At each point, a measurement was performed using a Mitutoyo SJ-210 surface roughness tester. Values for $\boldsymbol{R_a}$ (arithmetic mean surface roughness), $\boldsymbol{R_z}$ (maximum surface roughness), and $\boldsymbol{R_z}$ (total surface roughness) were recorded. The measurements were performed in a direction transverse to the grinding direction, and the average values for the five measurement points were calculated for each slab. See figure 26 for general overview of measurement points on the slabs.

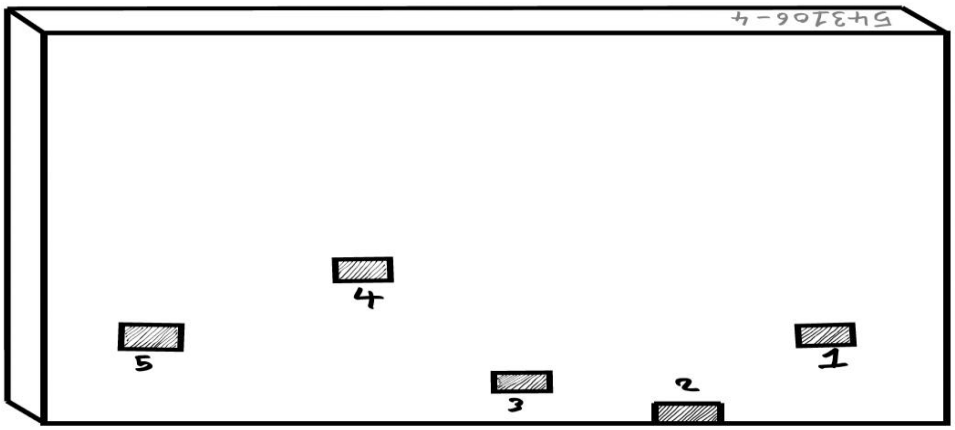

Figure 26: Example of a Map Showing Measurement Points on the Slab.

6.3 Slab sample preparation:

In this study, the surfaces of the two standard grinding routes used at Avesta Works today will be investigated, enabling a comparative analysis of surface properties following different processing methods. The two specific surface types to be examined are Hot-ground surface and Hot + cold-ground surface and cast (non-ground) surface, along with a cast surface where no grinding has taken place. These samples will be referred in the report as:

- Cast surface
- Hot Ground surface
- Hot+Cold Ground surface

Results from the investigation of these samples are presented in Chapter 7.3, where cross sections at the surface of these samples are analysed.

Figure 27: Example of Slabs Awaiting Cold Grinding.

The samples will be manufactured based on heat number 542862 and the slab dimension was 140 x 2070 mm, see Figure 28 for the positions of the slab samples taken. It is essential that the samples are produced in accordance with these specifications to ensure comparability and standardization of the obtained results from the grinding tests.

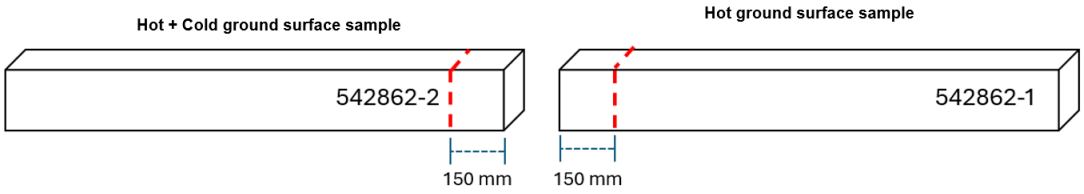

Figure 28: Position of the Samples on the Slabs.

After production, the cut slab samples were sent to the Outokumpu Avesta R&D Center for further sample preparation, see Figure 29.

Figure 29: Cut Slab Samples.

At the research center, the prepared slab samples will undergo further processing by first being divided into smaller units. These smaller units will then be cut to a standardized size of 25 x 20 mm using specialized cutting equipment. See Figure 30.

Figure 30: Standardized Sample Pieces.

After this initial cutting, the smaller pieces will undergo further processing using a more advanced cutting machine to be divided into even smaller units. This sequential processing aims to prepare the samples for precise analysis and advanced material investigations, enabling detailed characterization of the samples' properties at the micron level.

To process and analyze the material samples, a standardized encapsulation is performed using a hot press, see Figure 31. First, the press mold is filled with a conductive bakelite powder, and the material sample to be encapsulated is placed centrally within the mold.


Figure 31: Hot Press Used During the Project.

It is critical to ensure that the powder is evenly distributed and that the sample is correctly centered to achieve a defect-free result. The sample is then placed in a hot press. SimpliMet 1000, where pressure, temperature, and cycle time are set according to the specific requirements of the material, see Figure 32 and Figure 33.

Figure 32: Sample Pieces Correctly Centered in the Hot Press.

Figure 33: Powder Distributed Over the Sample Pieces in the Hot Press.

Once the preparations are complete, the process is activated, and the Bakelite powder melts, filling the space around the sample and encapsulating it. Upon cooling, the material hardens into a compact and durable block. The finished sample, Figure 34, is then removed from the press, with the smooth surface making it suitable for further processing, such as grinding, polishing, or microscopic analysis.

Figure 34: Fully Encapsulated Sample After Hot Pressing, Ready for Further Processing.

6.4 Sample Preparation, Metallographic:

To prepare metallographic samples for analysis, a precise and systematic polishing process is essential. In this work, the Saphir 550 machine was used, and the process was conducted in multiple steps with progressively finer grinding and polishing materials. The goal was to achieve a mirror-like, scratch-free surface, enabling the analysis of oxide layers in the cross-section of the samples.

The initial rough grinding was performed using Hermes P500 abrasive paper. With a machine setting of 80 N pressure for 1 minute, the samples were ground until the mounting material (Polyfast) and the sample surface were level. This procedure was repeated with a new abrasive paper to ensure that any remaining particles from the first paper were removed and a uniform surface was achieved. The grinding continued with Hermes P180 abrasive paper under the same settings, further leveling the surface. To ensure a scratch-free result, this process was repeated five times, each with a new abrasive paper.

After rough grinding, Hermes P320 abrasive paper was used to reduce scratches from previous steps. The grinding was repeated twice with 80 N pressure and a 1-minute working time for each pass. This was followed by two cycles with Hermes P500 abrasive paper, further reducing scratches and preparing the surface for finer grinding. Finally, Hermes P1000 abrasive paper was used for two more cycles with the same settings to achieve a smooth and fine surface. After each grinding step, the samples were thoroughly washed with water and soap to remove any grinding residues.

Following grinding, the polishing process began, replacing abrasive papers with polishing disks to minimize the risk of oxide damage. See Table 7 to Table 9 for information on each polishing step. Samples are fixated in a mounting unit so more samples can be made at the same time, see Figure 35.

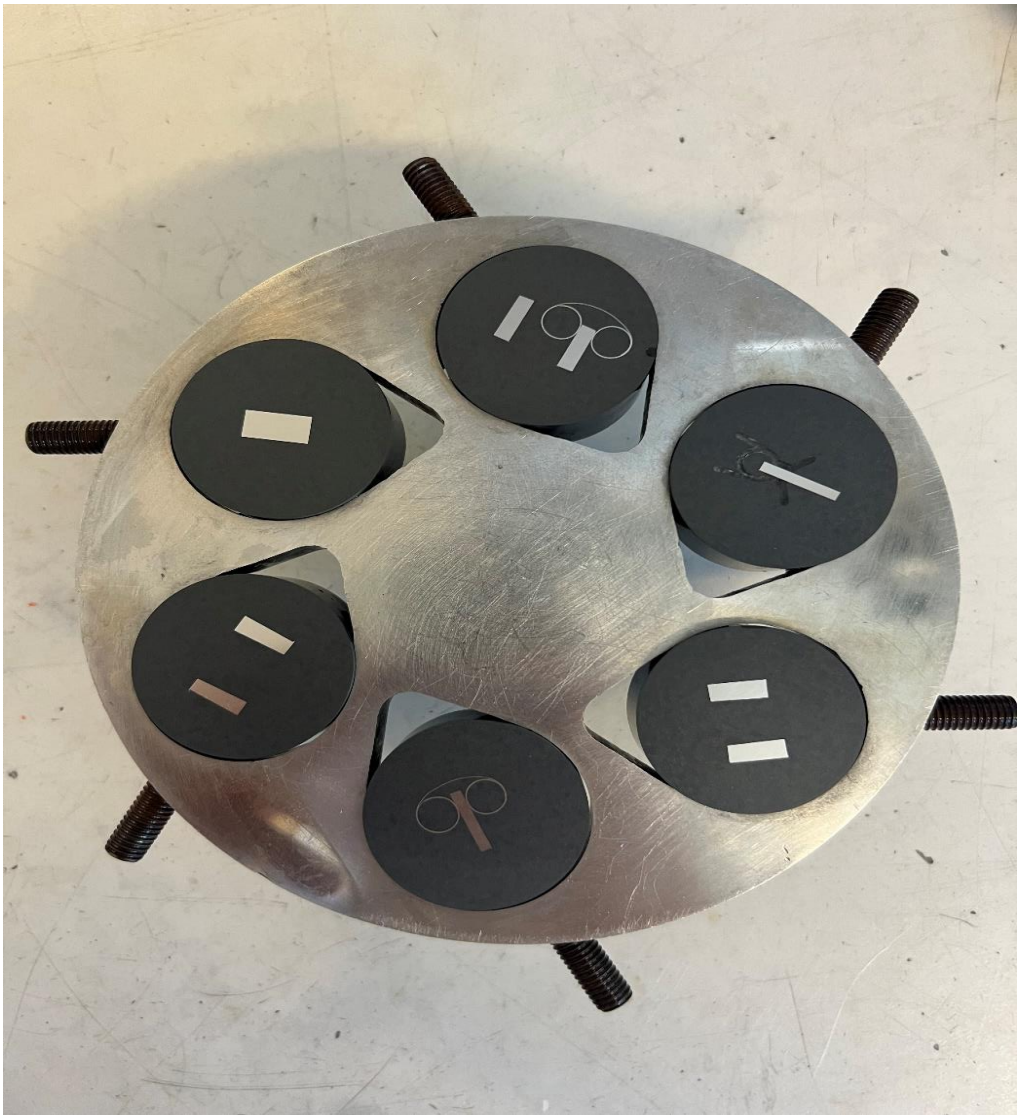

Figure 35: Multiple Encapsulated Sample Pieces Mounted for Polishing and Further Processing.

Table 7: First Polishing Step Details.

First polishing step	
Disk	MD-Allegro
Abrasive	Liquid Diamond 9-WY-XTAR
Lubricant	MetaDi™ Fluid
Settings	90 N pressure for 3 minutes, with the abrasive sprayed every 25 seconds and lubricant every 30 seconds.
Purpose	Create a mirror-like surface and eliminate scratches. If scratches were found, the step was repeated before the samples were thoroughly washed with water and soap in preparation for the next step

Table 8: Second Polishing Step Details.

Second polishing step	
Disk	MD-Mol
Abrasive	Liquid Diamond 3-WY-XTAR
Lubricant	MetaDi™ Fluid
Settings	90 N pressure for 4 minutes, with the abrasive sprayed every 30 seconds and lubricant every 35 seconds.
Purpose	Create a mirror-like surface and eliminate scratches. If scratches were found, the step was repeated before the samples were thoroughly washed with water and soap in preparation for the next step

A subsequent pass was conducted with the MD-Dac disk under the same settings for 2.5 minutes. Samples were washed thoroughly after this step.

Table 9: Final Polishing Step Details.

Final polishing step	
Disk	MD-Mol
Abrasive	Liquid Diamond 1-WY-XTAR
Lubricant	MetaDi™ Fluid
Settings	60 N pressure for 2 minutes, with the abrasive sprayed every 30 seconds and lubricant every 35 seconds.
Purpose	Ensure a mirror-like surface with minimal risk of oxide damage. If scratches were found, the step was repeated; otherwise, the process was concluded.

This methodical approach, using progressively finer grinding and polishing steps, produced high-quality, scratch-free surfaces suitable for detailed analysis of the surface layer oxides in the sample cross-sections.

7 Results

7.1 Surface Roughness Measurements of Production Slabs:

Before conducting measurements on the three selected slabs, several preliminary measurement tests were performed on a total of ten slabs. These tests ensured the correct use of the measuring instrument and provided an opportunity to learn the exact measurement procedure. Test measurements were conducted on both hot- and cold-ground materials and provides reference values for the surface roughness obtained with the current production route at Avesta Works. 6 slabs of each grinding route were measured.

Figure 36 shows the measured surface roughness (Ra- and Rz-values, along with standard deviation) for Hot and Cold Ground slabs, respectively.

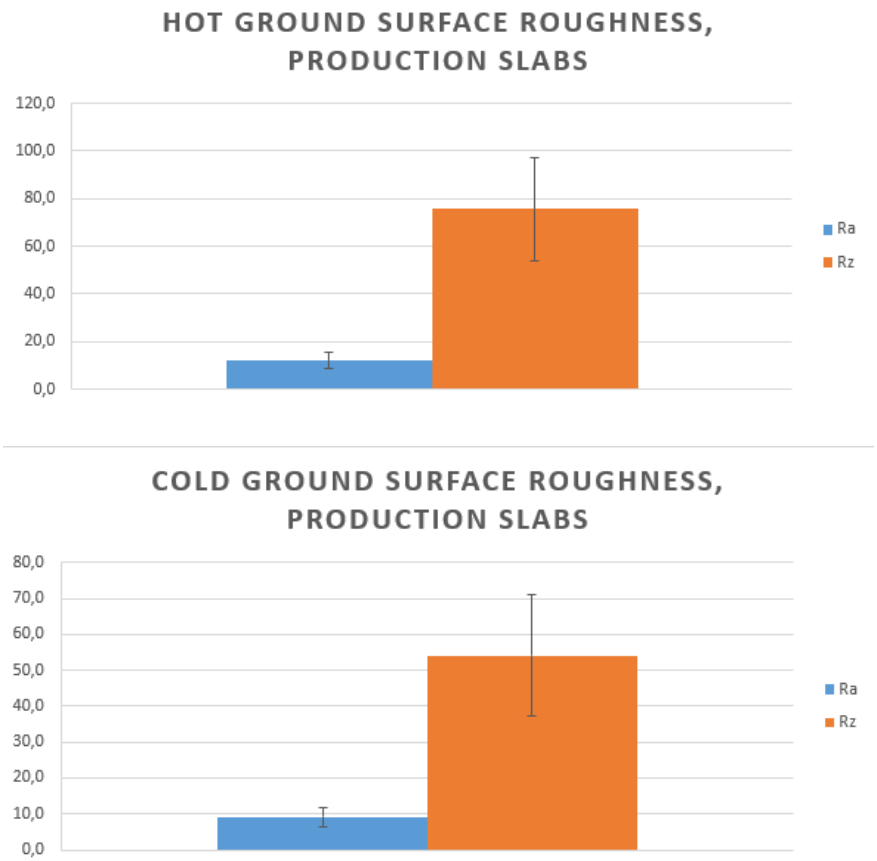

Figure 36: The cold and hot ground surface roughness for production slabs.

When comparing Ra and Rz-values between Hot- and Cold Ground surfaces, it is seen that cold ground surfaces gives a slightly finer surface, see Figure 37.

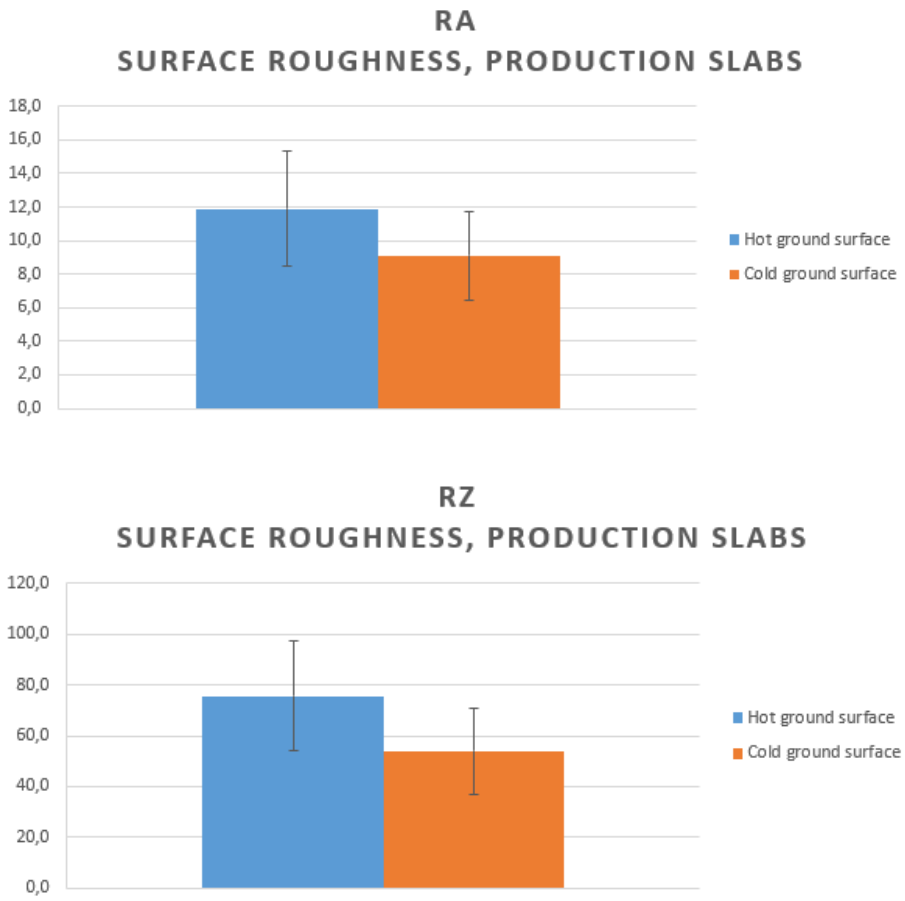

Figure 37: Ra and Rz surface roughness for production slabs.

7.2 Surface Roughness with New Cold Grinding Methods

The results, presented in table form, display the various values of arithmetic mean surface roughness R_a , which defines the average distance between the peaks and valleys of the surface profile over a specified length. The lower the R_a value, the smoother the surface. In contrast, maximum surface roughness R_z describes the total roughness profile, focusing on the maximum variation in the surface profile. Similarly, a lower R_z value indicates a smoother surface.

Method 1:

Table 12: Test Results for Sample 1

Sample 1												
Standard: ISO 1997												
	Sample: non-ground		**Sample: Rough (Lower)**		**Sample: Fine (Lower)**		**Sample: non-ground**		**Sample: Rough (Upper)**		**Sample: Fine (Upper)**	
	Ra	**Rz**	**Ra**	**Rz**	**Ra**	**Rz**	**Ra**	**Rz**	**Ra**	**Rz**	**Ra**	**Rz**
Area 1	14.9	77.4	4.7	32.3	8.6	48.6	12.4	64.1	12.0	73.6	10.5	66.2
Aera 2	11.6	80.4	9.3	63.4	12.1	64.3	9.4	64.1	13.5	79.2	10.9	63.1
Area 3	8.3	56.3	6.3	40.1	9.8	57.5	8.0	56.6	8.0	48.4	6.9	38.7
Area 4	17.8	82.8	15.8	77.1	6.0	32.9	15.1	80.1	10.4	57.1	12.1	73.6
Area 5	12.6	91.8	16.8	95.3	5.6	33.7	14.1	95.6	16.5	88.6	9.8	52.2
Cut-off	2.5		2.5		2.5		2.5		2.5		2.5	

Sampling speed*	0.5	0.5	0.5	0.5	0.5	0.5
$\lambda c = 2.5$		$\lambda c = 2.5$		$\lambda c = 2.5$		

Method 2:

Table 13: Test Results for sample 2.

Sample 2												
Standard: ISO 1997												
	Sample: non-ground		**Sample: Rough (Upper)**		**Sample: non-ground**		**Sample: Rough (Lower)**		**Sample:**		**Sample:**	
	Ra	**Rz**	**Ra**	**Rz**	**Ra**	**Rz**	**Ra**	**Rz**	**Ra**	**Rz**	**Ra**	**Rz**
Area 1	9.7	71.4	6.5	35.9	12.4	80.1	8.3	49.3				
Aera 2	9.8	65.0	8.3	56.2	8.7	64.4	6.4	41.1				
Area 3	10.1	65.9	3.4	22.7	14.5	90.1	14.1	88.9				
Area 4	9.1	55.2	13.2	79.4	13.1	89.1	6.3	36.2				
Area 5	12.7	89.6	6.9	37.1	13.9	81.3	12.1	75.1				
Cut-off	2.5		2.5		2.5		2.5					
Sampling speed*	0.5		0.5		0.5		0.5					
$\lambda c = 2.5$			$\lambda c = 2.5$				$\lambda c = 2.5$					

Method 3:

Table 14: Test Results for sample 3.

Sample 3												
Standard: ISO 1997												
	Sample: non-ground		**Sample: Rough (Lower)**		**Sample: Fine (Lower)**		**Sample: non-ground**		**Sample:**		**Sample:**	
	Ra	**Rz**	**Ra**	**Rz**	**Ra**	**Rz**	**Ra**	**Rz**	**Ra**	**Rz**	**Ra**	**Rz**
Area 1	9.1	53.4	10.3	63.9	10.6	69.1	13.9	88.8				
Aera 2	6.7	38.2	7.3	48.2	12.1	89.6	13.9	83.5				
Area 3	15.4	99.7	11.2	67.2	14.0	82.0	13.7	78.2				
Area 4	13.9	84.7	13.0	71.4	24.7	154.1	12.8	80.6				
Area 5	11.4	73.4	12.0	66.7	11.5	95.6	16.8	121.6				
Cut-off	2.5		2.5		2.5		2.5					
Sampling speed*	0.5		0.5		0.5		0.5					
$\lambda c = 2.5$			$\lambda c = 2.5$				$\lambda c = 2.5$					

7.3 Analysis of cross sections

This section presents the results of the current slab surface obtained in the production processes at Avesta Works (as presented in 6.3). Section 7.3.1 shows the cross section from a cast (non-ground) surface and its characteristics.

7.3.1 The cross section from a cast (non-ground) surface

The examination showed that the oxide on top of the slab surface likely is mixed with various amounts of casting powder (e.g. CaO, Al_2O_3, MgO, Na_2O, SiO_2 and F). Traces of F was also possibly present but since F is interfered by Fe it is difficult to analyze. Due to this, F was removed from the EDS analysis. Another element that should be evaluated with care is Si. Sample cross sections are polished in SiO2 and Si will therefore always be present in cavities since there are many small cavities in an oxide. Element maps and EDS analysis are shown below but note that the analysis shall be considered as qualitative rather than quantitative.

Figure 38: Cast surface (non-ground slab)

The oxide/casting powder mixture is relatively thin, 5 – 200 µm. The innermost oxide/casting powder mixture is slightly denser than the outermost mixture. The denser thin oxide mixture (~ 5-10 µm) covers the whole slab surface (best seen to the very left in Figure 35 as a darker grey thin film on top of the, in the image, light grey bulk). Only at a one location a thicker (~ 200 µm) and more porous oxide/casting powder mixture is present above the thinner layer, see Figure 35 below. Since the oxide is relatively thin, oxide thickness measurements are no good measurements for how much grinding should occur on a slab surface. The slab surface is very uneven, “wavy” (seen already with the eye). Due to the un-even surface, removing 200 µm of the slab surface wouldn´t remove the oxide present in the valleys of the “wavy” slab surface. Further, surface studies revealed that oxide/casting powder mixture is

present also in the bulk, see example in Figure 39 below. The oxide/casting powder mixture in the bulk must of course also be removed.

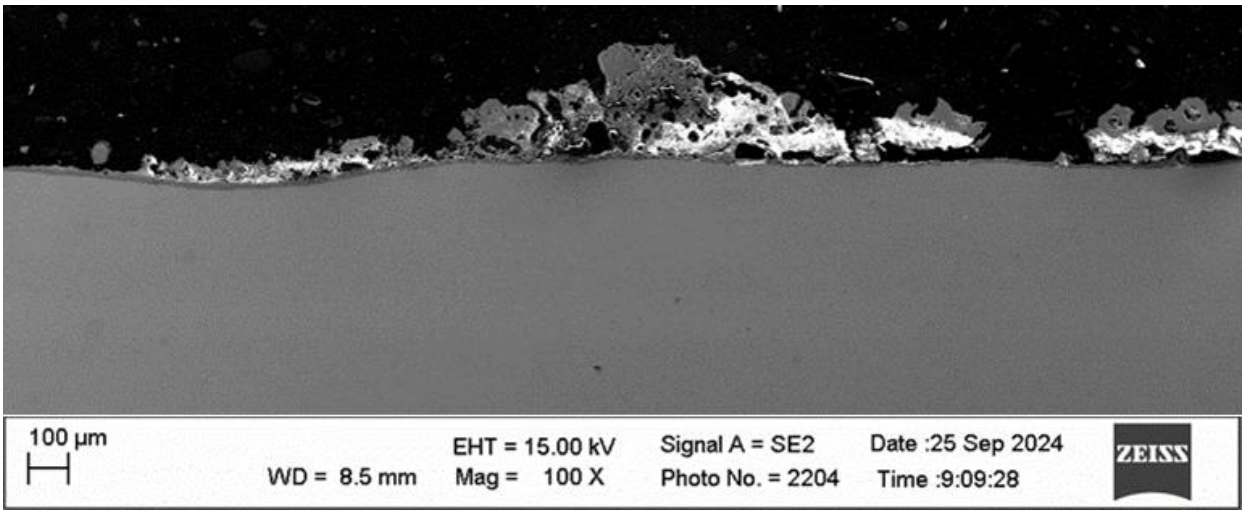

Figure 39: Duplex 2205 cross section of oxide, at a location with thicker oxide, magnification 100X.

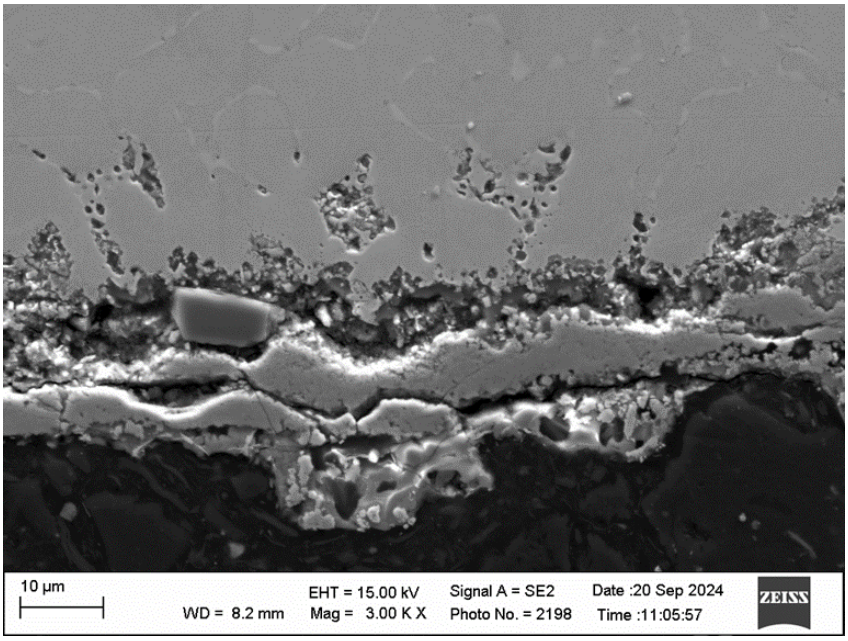

Figure 40: Oxide/casting powder mixture present in the bulk

7.3.2 Oxide/casting powder composition on the Duplex 2205 slab surface (cast surface)

The analysis revealed that the surface of the Duplex 2205 plate consists of various layers of oxide and casting powder with differing compositions. Examples of these layers, along with their chemical content, are presented in Figure 40 to 44 Figure below.

The information provided is based on conducted analyses and should be regarded as a qualitative overview of the composition of the layers. The results offer a clear understanding of the differences observed between the layers, which is valuable for comprehending their formation and potential impact on the plate's surface.

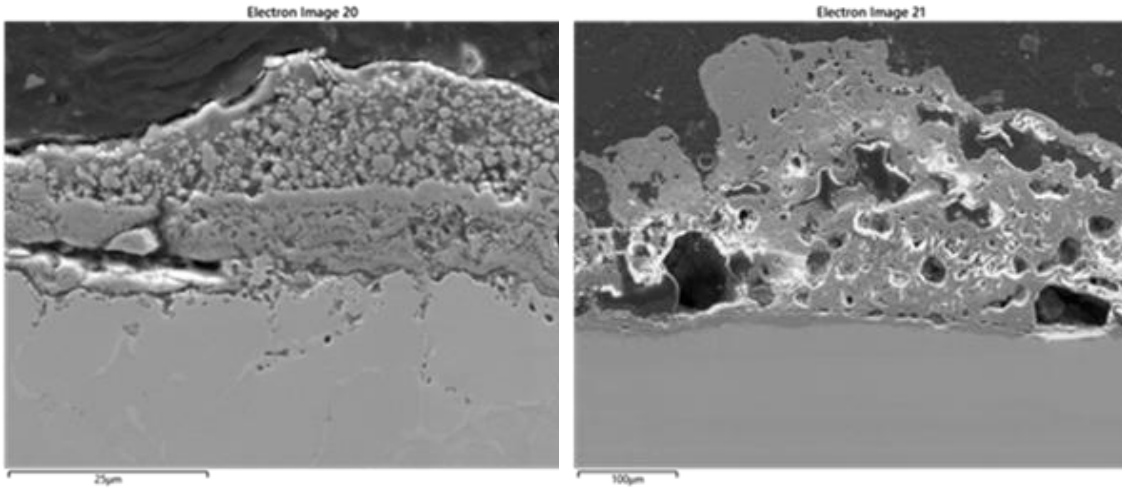

Figure 41: Example of oxide/casting powder layers on a Duplex 2205 slab surface. Oxide/casting powder mixture < 25 µm thick (left image) and oxide/casting powder mixture ~ 200 µm thick (right image).

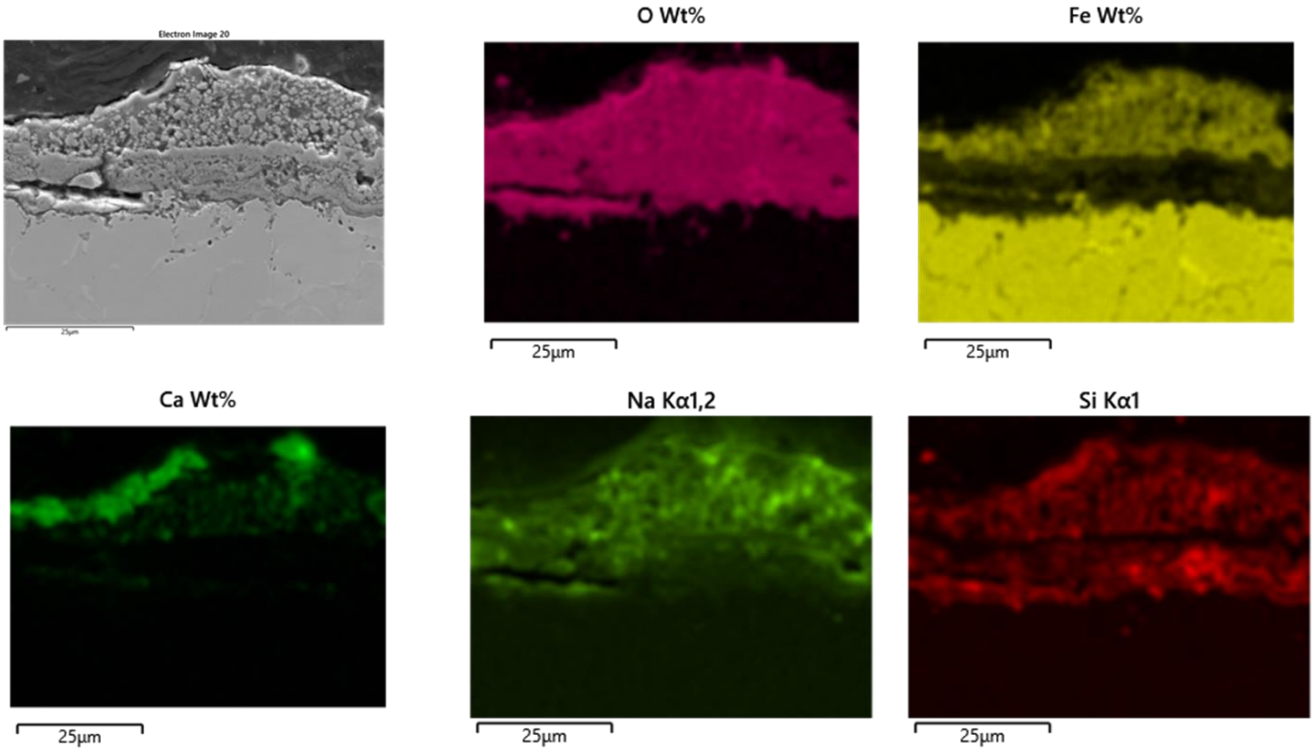

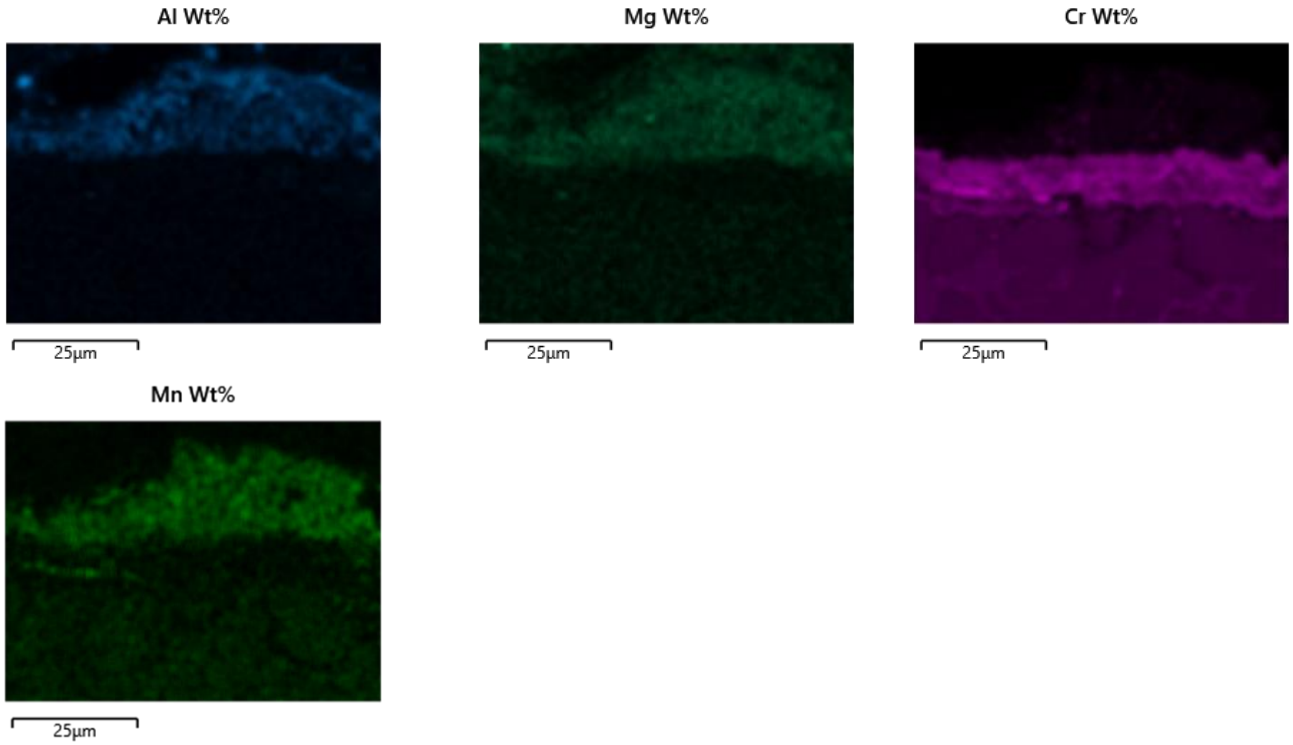

Figure 42: Element maps, 15kV EDS. Inner oxide layer is mainly enriched in Cr, outer layer is mainly enriched in Mn, Al, Mg and Ca. Na is more widely spread.

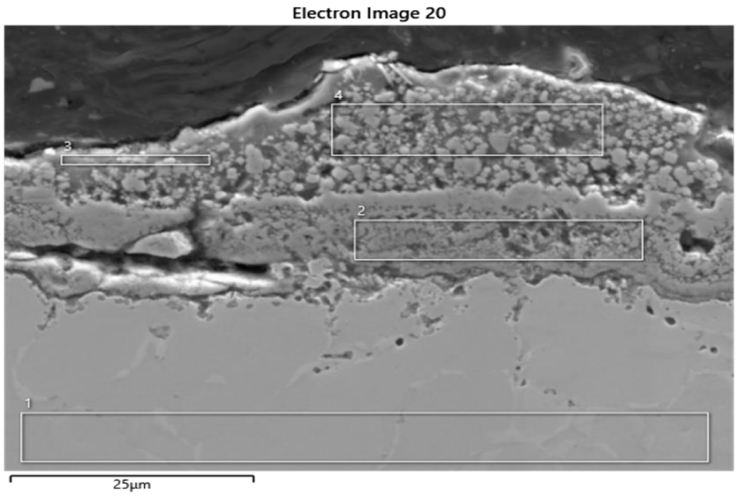

Figure 43: Cross section of Duplex 2205 slab surface at a section with a slightly thicker oxide/casting powder mixture (< 25 µm), see EDS analyzation results in Table 1 below. Thickness < 25 µm.

The results presented in Table 15 provide an overview of the elemental composition across four analyzed surface regions. Spectrum 1 shows a surface dominated by iron (61.7 wt%) and chromium (22.0 wt%), with low oxygen content (4 wt%), suggesting minimal oxidation. In Spectrum 2, the oxygen level increases significantly to 33 wt%, alongside a higher chromium content (37.7 wt%), indicating a more oxidized surface layer. Spectrum 3 reveals a notable presence of oxygen (36 wt%) and silicon (16.4 wt%), suggesting a mixed oxide layer with reduced levels of chromium and iron compared to Spectrum 1. Lastly, Spectrum 4 shows elevated levels of oxygen (33 wt%), aluminum (7.1 wt%), and magnesium (5.18 wt%), likely reflecting the presence

of casting powder residues. These differences in composition reflect the varying surface characteristics influenced by processing conditions.

Table 15: EDS analyzation results, see analyzation sites in Figure 43 above. 15kV, normalized results (wt%)

Spectrum	C	O	Na	Mg	Al	Si	Ca	Cr	Mn	Fe	Ni	Mo
1	4*	< 1	-	-	0,2	0,9	-	22,0	1,4	61,7	5,7	3,0
2	7	33	0,76	< 0,2	0,3	9,2	0,2	37,7	-	8,5	2,8	1,5
3	23	36	1,58	0,3	1,3	5,2	16,4	1,2	0,9	12,8	0,7	< 0,2
4	8	33	5,18	0,7	1,7	7,1	3,9	5,6	2,4	32,0	1,2	< 0,2

*Peak of C is always present in EDS spectra even though no C is present

The high C signal in spectrum 3 is likely Polyfast which was used for hot mounting of the specimens. When zooming in on the two oxide layers, a clear boundary between the inner and outer layer is seen, see Figure 44 below.

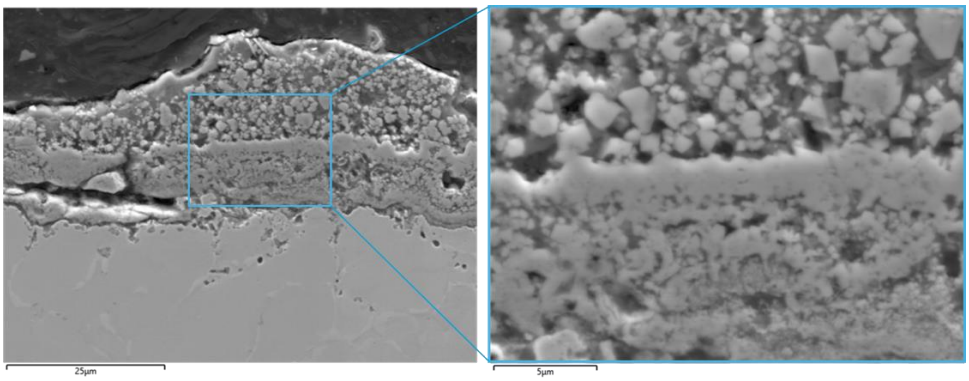

Figure 44: Oxide and casting powder mixture at Duplex 2205 slab surface, total thickness < 25 µm.

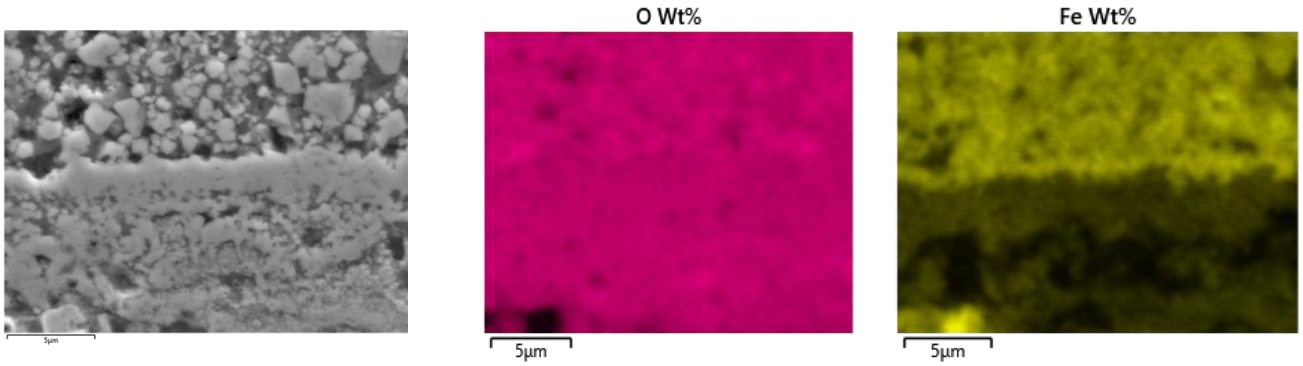

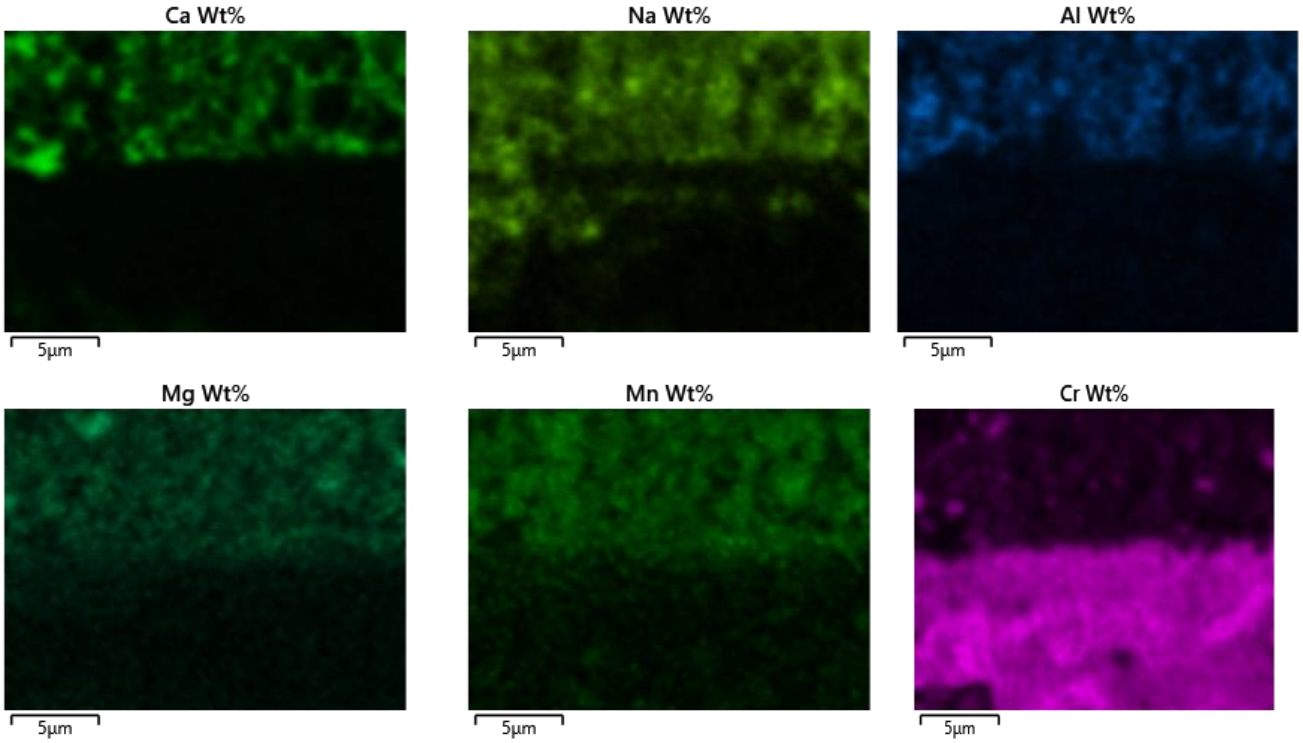

Figure 45: As in the maps in Figure 4, elements from casting powder (outer layer) and mainly Cr oxide (inner layer)

The spectrum and EDS results obtained from the analysis are presented in Figure 46 and Table 16 below. These results provide an overview of the elements identified in the sample and their relative abundance within the analyzed area.

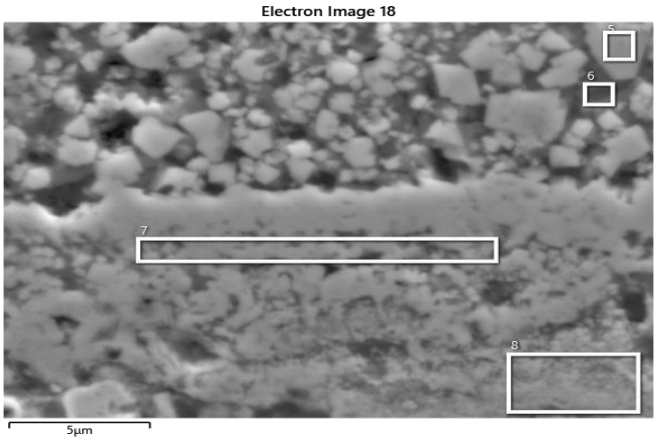

Figure 46: Oxide and casting powder mixture at Duplex 2205 slab surface

The results in Table 16 describe the elemental composition of four surface regions, highlighting differences in material characteristics. Spectrum 5 shows oxygen at 32 wt% and sodium at 4.2 wt%, along with moderate amounts of chromium (7.7 wt%) and iron (36.4 wt%), indicating an oxidized surface with mixed compounds. Spectrum 6 has a slightly higher oxygen content (35 wt%) and sodium (9.6 wt%), combined with increased silicon (11.8 wt%) and calcium (5.1 wt%), suggesting the presence of oxides or surface residues. Spectrum 7 contains lower oxygen levels (31 wt%) and reduced chromium (38.4 wt%) and iron (14.5 wt%), which may reflect a less oxidized surface. Spectrum 8, with oxygen at 30 wt%, also includes higher molybdenum (5.2 wt%) and chromium (33.7 wt%), likely indicating influence from alloying elements or

process residues. These variations in composition suggest that surface conditions are influenced by the specific manufacturing processes applied.

Table 16: EDS analyzation results, see analyzation sites in Figure 46 above. 15kV, normalized results (wt%)

Spectrum	C	O	Na	Mg	Al	Si	Ca	Cr	Mn	Fe	Ni	Mo
5	5*	32	4,2	1,1	1,4	5,0	2,7	7,7	3,2	36,4	1,6	<0,2
6	5	35	9,6	0,4	2,6	11,8	5,1	4,6	1,3	24,2	0,6	<0,2
7	6	31	1,8	<0,2	0,3	4,0	0,2	38,4	0,6	14,5	2,5	0,8
8	6	30	0,0	<0,2	<0,2	7,0	<0,2	33,7	<0,2	12,6	4,6	5,2

*Peak of C is always present in EDS spectra even though no C is present

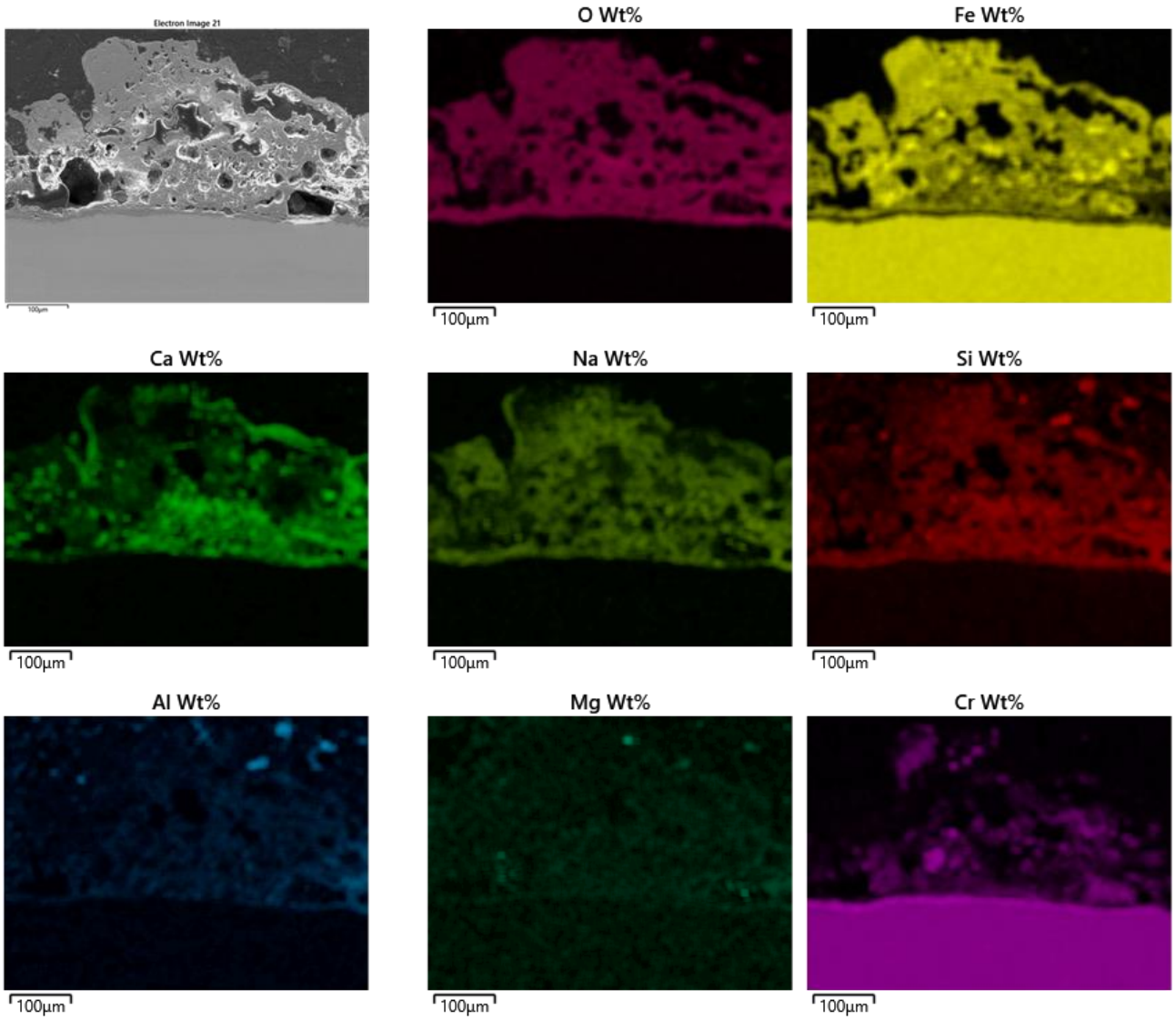

Figure 47: Cross section of a thicker (~ 200 µm) oxide/casting powder mixture on the slab surface.

The thicker, porous oxide/casting powder mixture had many larger cavities (holes). After sample preparation, most of the cavities were filled with Polyfast from hot mounting (i.e. carbon, C, which is not shown in the figure above).

The spectrum and EDS results obtained from the analysis are presented in Figure 48 and Table 17 below. These results provide an overview of the identified elements and their occurrence in the examined mixture.

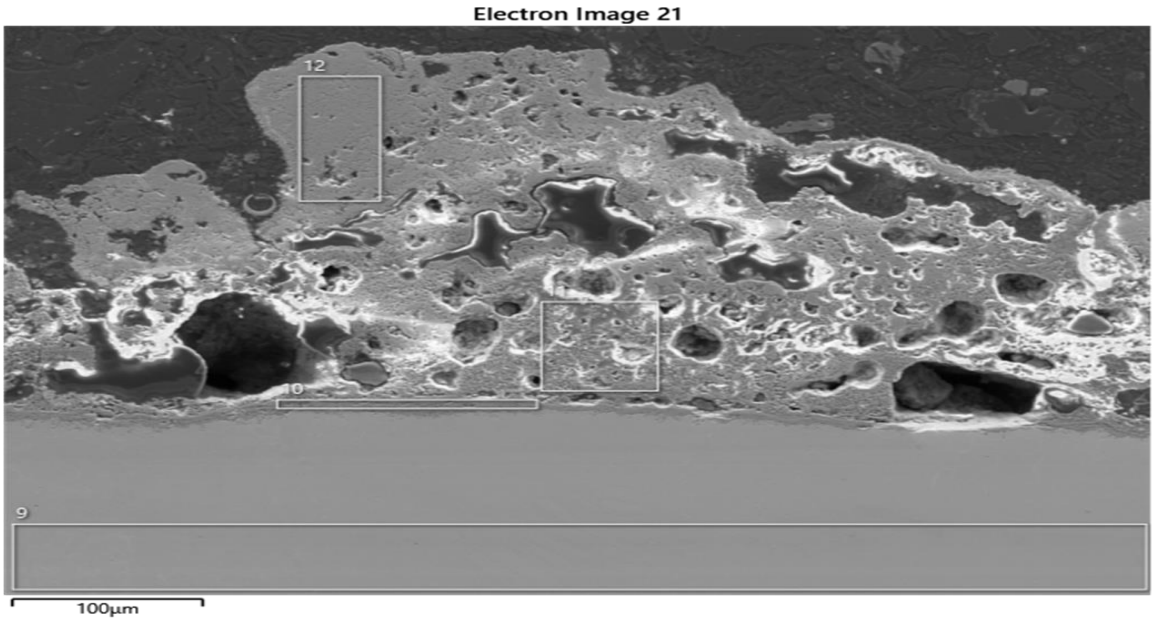

Figure 48: Cross section of a thicker (~ 200 µm) oxide/casting powder mixture on the slab surface.

The results presented in Table 17 show the elemental composition of four surface regions. Spectrum 9 has a low oxygen content (4 wt%) and a high concentration of iron (62.9 wt%), along with chromium (22.6 wt%), which suggests a predominantly metallic surface with limited oxidation. Spectrum 10 displays higher oxygen levels (31 wt%) and sodium (3.2 wt%), with chromium (26.9 wt%) and iron (23.3 wt%), indicating the presence of oxides and possible residues from the manufacturing process. Spectrum 11 contains elevated oxygen (33 wt%), silicon (7.4 wt%), and calcium (11.8 wt%), suggesting a mixed oxide layer likely formed due to surface reactions. Spectrum 12 shows moderate oxygen content (28 wt%) and calcium (2.2 wt%), with reduced chromium (10 wt%) and significant iron levels (53 wt%), which could reflect a surface influenced by alloy composition. These variations highlight differences in surface composition resulting from processing conditions.

Table 17: EDS analyzation results, see analyzation sites in Figure 48 above. 15kV, normalized results (wt%)

Spectrum	C	O	Na	Mg	Al	Si	Ca	Cr	Mn	Fe	Ni	Mo
9	4*	< 1	-	-	< 0,2	0,4	-	22,6	1,5	62,9	5,5	3,0
10	6	31	3,2	-	0,4	4,2	0,6	26,9	0,8	23,3	3,4	0,5
11	9	33	3,8	0,3	0,8	7,4	11,8	2,4	1,2	29,4	1,1	0,0
12	7	28	2,4	< 0,2	0,4	2,2	1,0	4,3	0,3	53,0	0,7	0,3

*Peak of C is always present in EDS spectra even though no C is present

7.3.3 Surface Analysis of hot ground surface

The surface of a hot ground slab was analyzed to determine its composition and characteristics. The results of the analysis are presented in Figure 49 to Figure 52, focusing on the observed oxide or casting powder layers. The investigation includes both the surface layers and any underlying structures, aiming to provide a more comprehensive understanding of the material's properties and potential variations in the composition and structure of the layers.

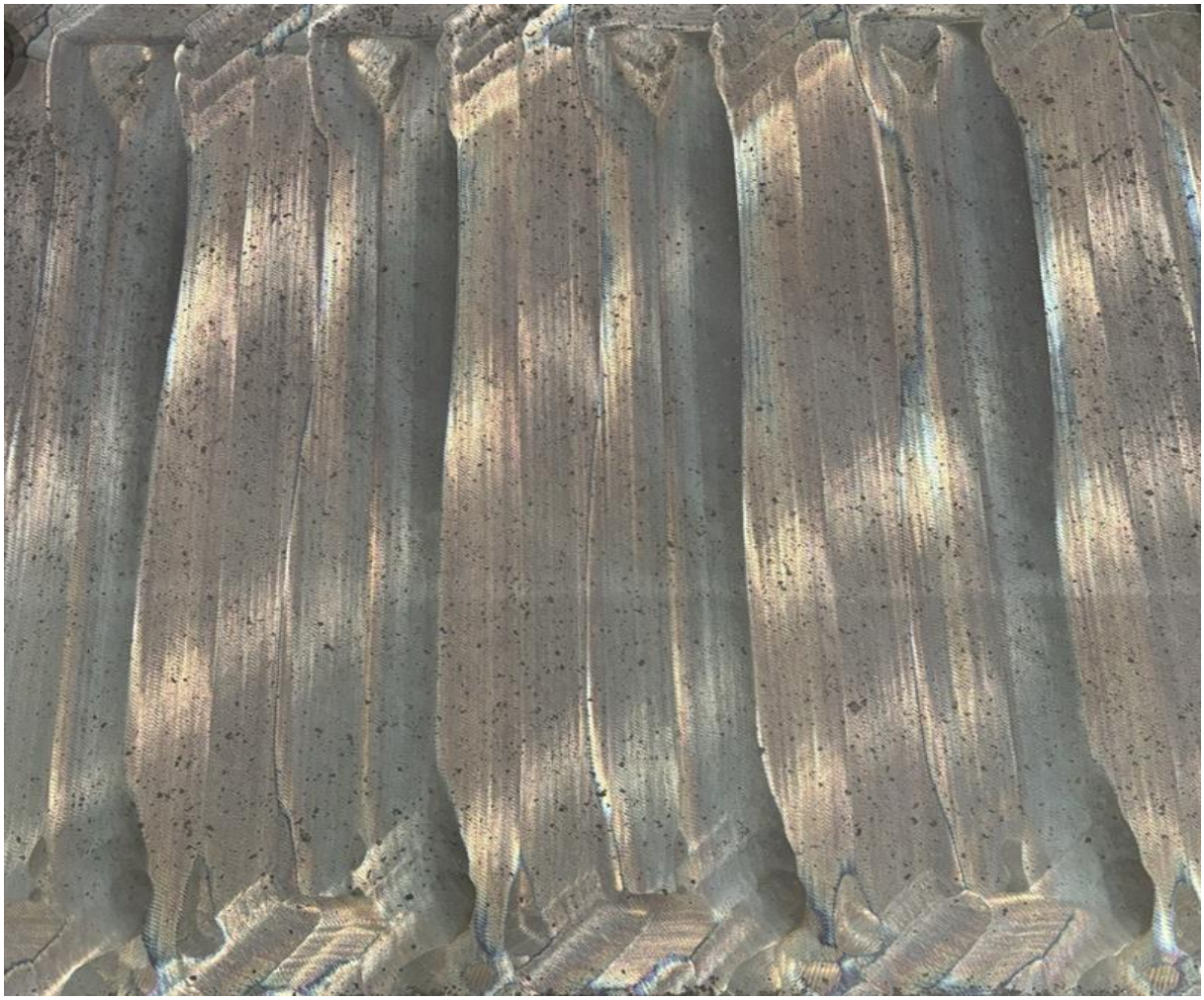

Figure 49: Cast surface (hot ground surface)

This analysis provides valuable insights into the material's behavior, which can inform further assessments or processing improvements.

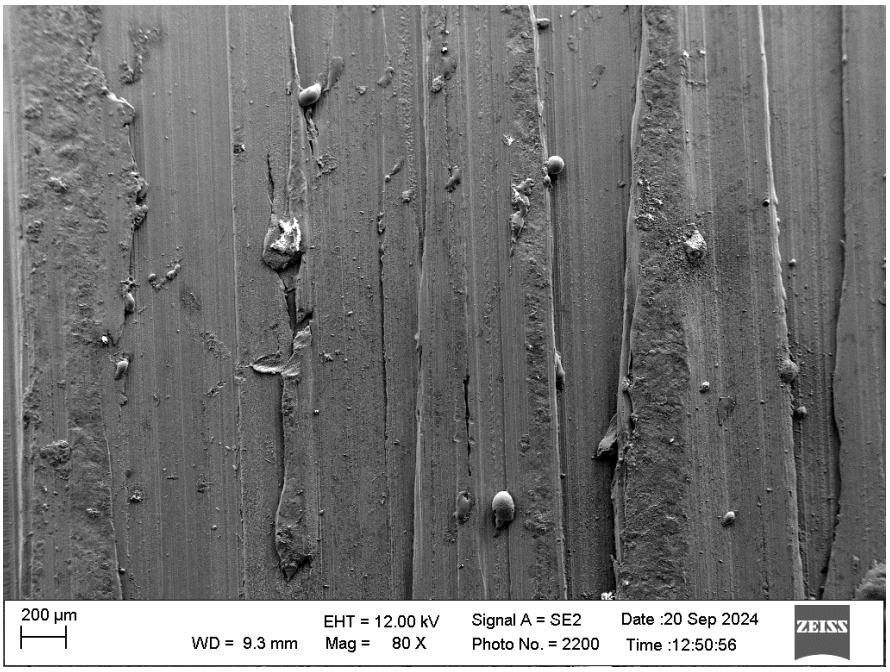

Figure 50: Sample 2 surface, FEG-SEM image, SE detector 12 kV.

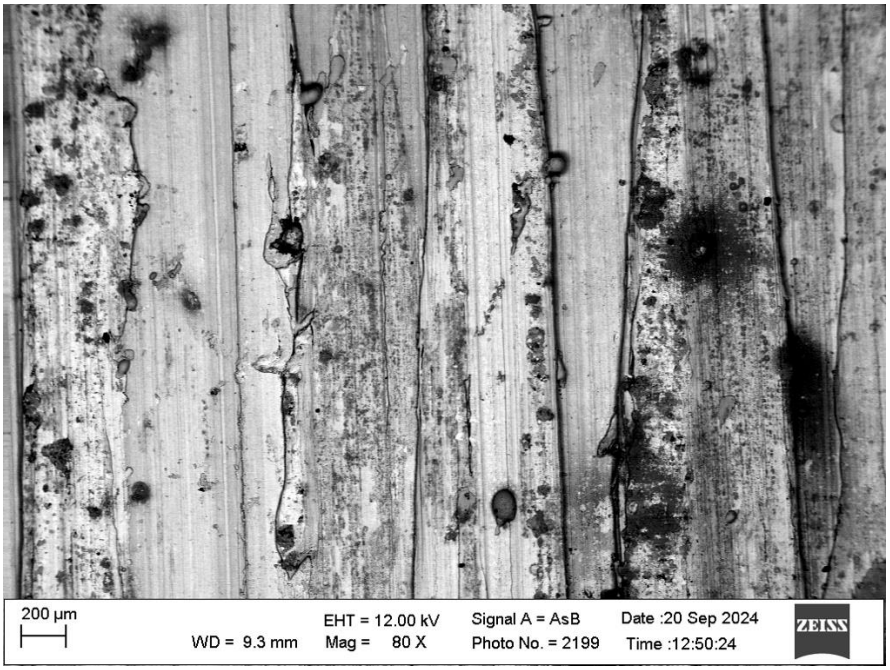

Figure 51: Sample 2 surface, FEG-SEM image, BS (back scatter) detector 12 kV.

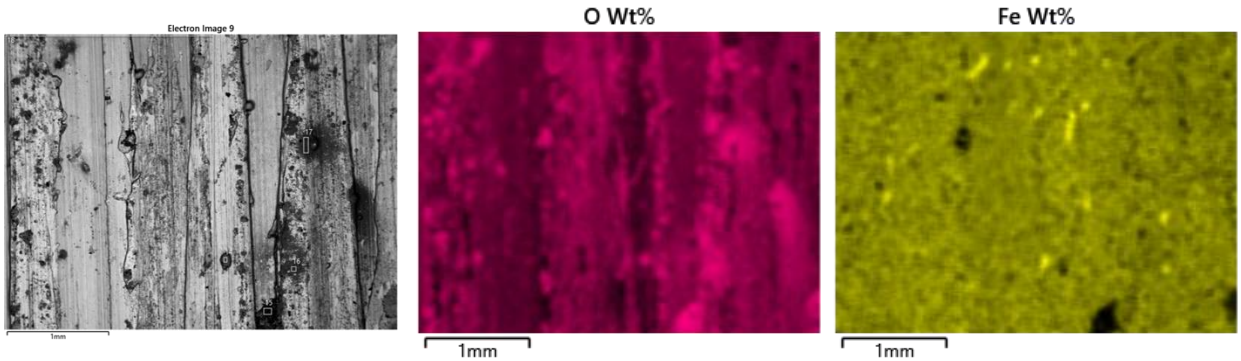

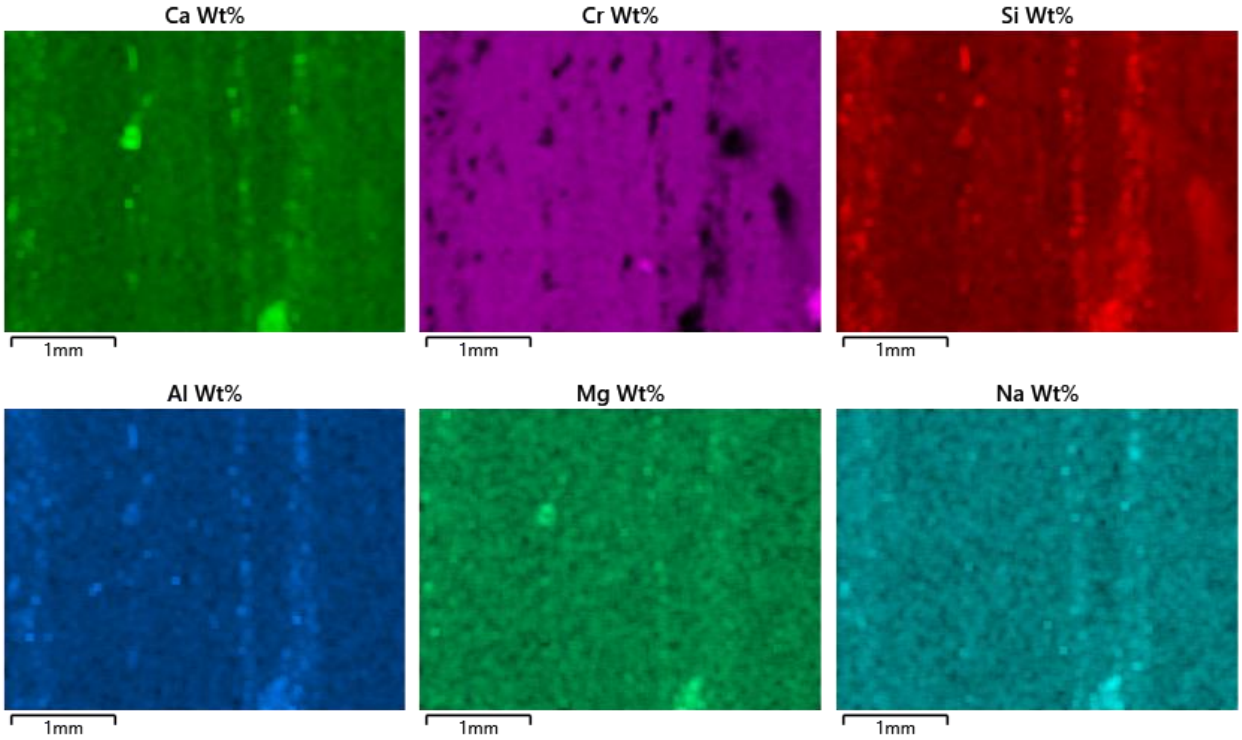

Figure 52: Sample 2, EDS map, 12kV. Casting powder remaining on top of the slab surface.

Figure 53: Sample 2, backscatter detector, 12kV, EDS results are shown in Table 4-18 below.

The data in Table 18 provide the elemental composition of five surface regions (selected spectrums shown in Figure 49), reflecting variations influenced by processing conditions. Spectrum 14 shows oxygen at 27 wt%, chromium at 29.4 wt%, and iron at 40.2 wt%, indicating an oxidized surface with metallic components.

Spectrum 15 includes higher carbon (28 wt%) and oxygen (32 wt%), along with calcium (14.7 wt%) and lower iron (10.3 wt%), which may suggest organic contamination and residues from casting powder. Spectrum 16 exhibits elevated oxygen (33 wt%) and silicon (3.9 wt%) with reduced chromium (7.4 wt%), suggesting the presence of surface oxides or residues. Spectrum 17 has similar oxygen levels (32 wt%) but higher iron (61 wt%), pointing to a surface dominated by metallic elements and oxidation. Finally, Spectrum 18 shows lower oxygen (13 wt%) and chromium (19.1 wt%) with significant iron content (58.5 wt%), indicating a metallic surface with minimal oxide formation. These results highlight how processing methods, such as grinding and casting, influence the surface composition.

Table 18: EDS analysis results, 12kV, normalized results, see location of spectrums in Figure 53 above.

Spectrum	C	O	Na	Mg	Al	Si	Ca	Cr	Mn	Fe	Ni	Mo
14	-	27	0,3	-	0,3	0,4	0,4	29,4	0,7	40,2	<0,2	1,5
15	28	32	1,2	0,6	1,4	4,6	14,7	1,5	1,2	10,3	3,9	0,6
16	-	33	0,3	<0,2	<0,2	3,9	0,7	4,4	<0,2	55,5	0,6	1,5
17	-	32	<0,2	<0,2	<0,2	1,6	0,6	1,8	<0,2	61,0	0,6	1,8
18	-	13	-	<0,2	<0,2	0,6	0,3	19,1	1,2	58,5	4,7	2,8

The high oxygen, O, content on the surface could possibly be oxide caused by heat development during grinding. The high C signal in spectrum 15 might be some organic contamination. Traces from casting powder are seen in some spectrums. This shows that a hot ground surface might not be completely free from casting powder and other surface contamination.

7.3.4 Surface Analysis of Hot + Cold ground surface sample

The surface of a Hot+cold ground slab was examined to study its composition and structure. The analysis focuses on the oxide or casting powder layers identified, including their variations in thickness and composition.

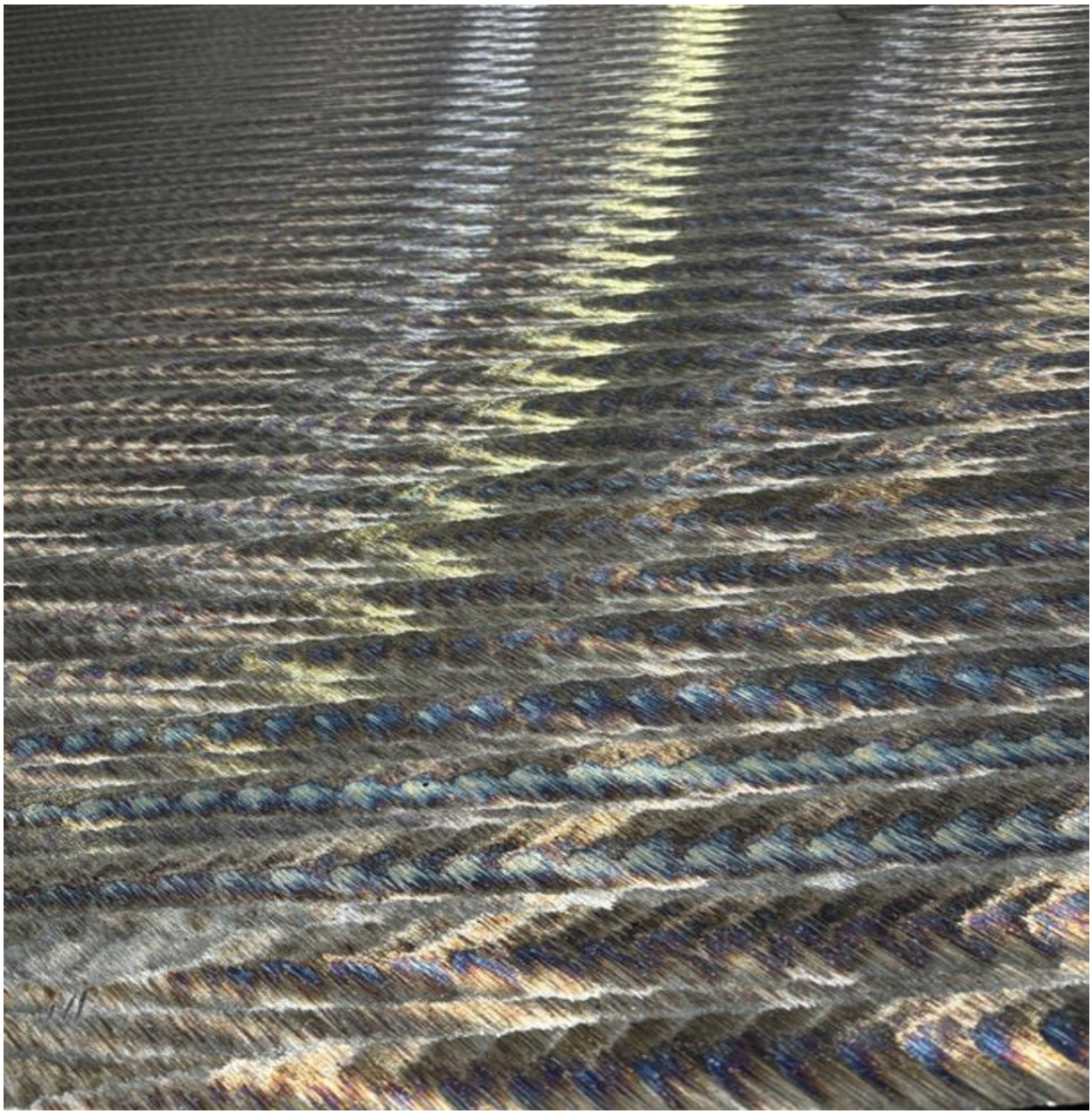

Figure 54: Hot + Cold ground surface, 45°

The results are presented in Figure 59 to Figure 62, providing an overview of the material's surface properties. The investigation includes both the surface layer and any underlying layers to gain a deeper understanding of the material's structure and characteristics.

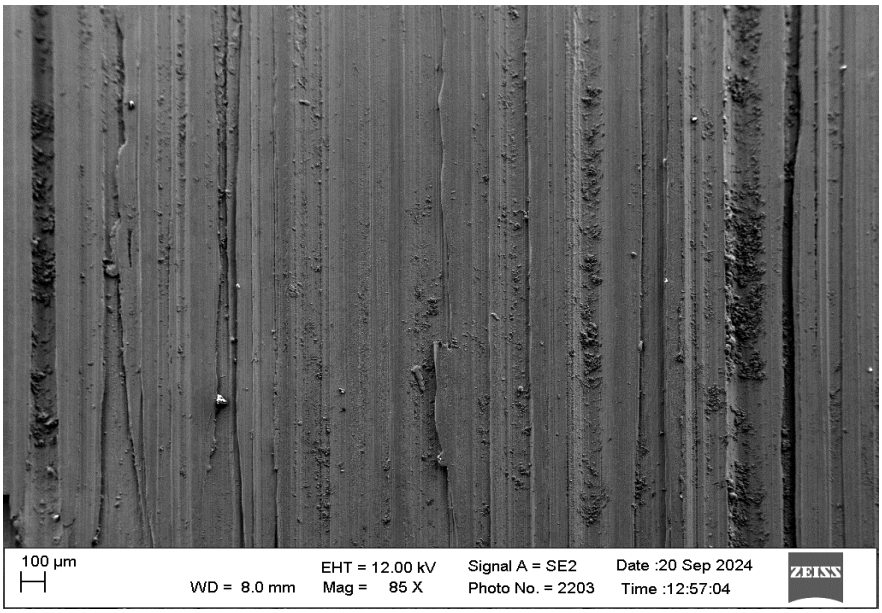

Figure 55: Sample 3 surface, FEG-SEM image, SE detector 12 kV.

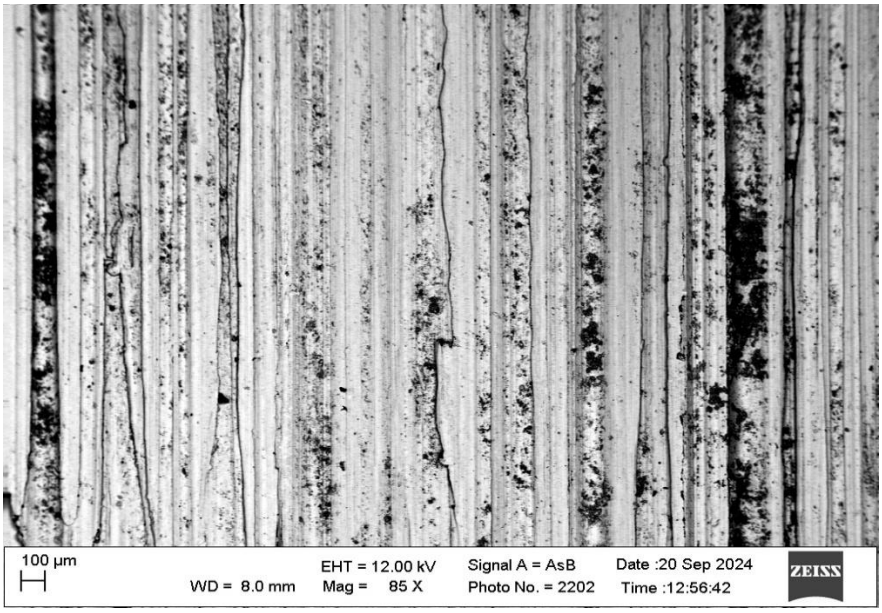

Figure 56: Sample 3 surface, FEG-SEM image, BS (back scatter) detector 12 kV.

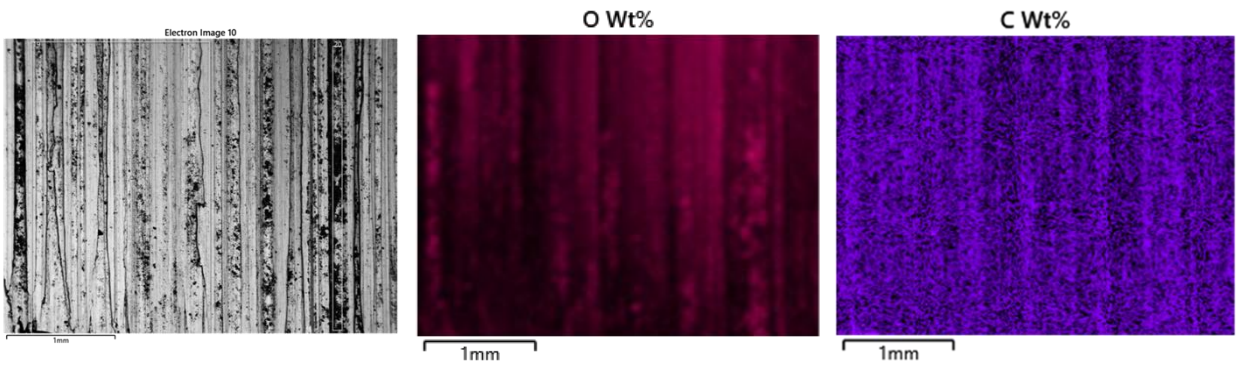

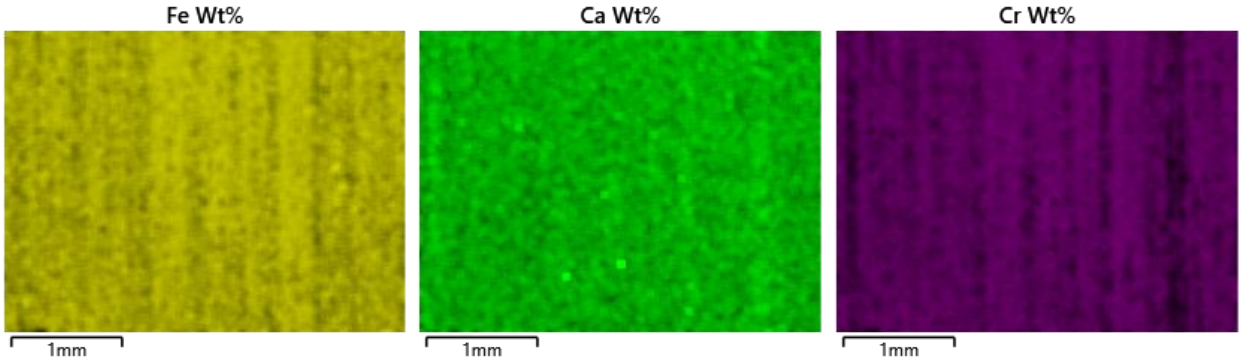

Figure 57: Sample 3, EDS map, 12kV.

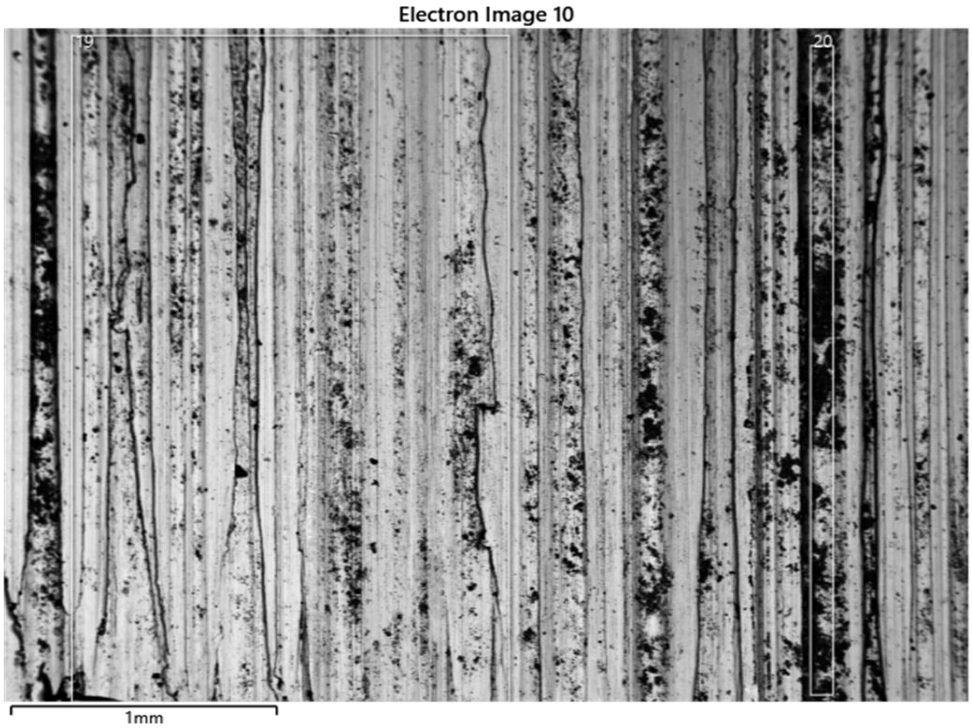

Figure 58: Sample 3, backscatter detector, 12kV, EDS results are shown in Table 5 below.

Table 19 shows the elemental composition of two shallow surface regions analyzed at 12 kV (location of spectrums are shown in Figure 52). Spectrum 19 has 6 wt% oxygen and 20.9 wt% chromium, along with a high iron content (62.9 wt%) and smaller amounts of nickel (5.1 wt%) and molybdenum (2.9 wt%). This indicates a mostly metallic surface with minimal oxidation. Spectrum 20, on the other hand, shows higher oxygen levels (12 wt%) and lower chromium (15.7 wt%), with increased iron content (65.1 wt%), as well as nickel (3.4 wt%) molybdenum (1.7 wt%). The higher oxygen content in Spectrum 20 suggests more surface oxidation, possibly due to differences in treatment or environmental exposure. These results highlight variations in surface composition caused by processing and external conditions.

Table 19: EDS analysis results, 12kV for shallow surface analysis. Normalized results, wt%. Analyzation sites are seen in Figure 58 above.

Spectrum	O	Na	Mg	Al	Si	Ca	Cr	Mn	Fe	Ni	Mo
19	6	-	<0,2	<0,2	0,4	<0,2	20,9	1,3	62,9	5,1	2,9
20	12	-	<0,2	0,2	0,5	0,3	15,7	1,1	65,1	3,4	1,7

Carbon, C, is not displayed in the table above due to unexpected contamination during analysis. C was removed before normalization of the results. Even though the C content couldn't be analyzed, more C was however found in spectrum 20 compared to spectrum 19, compare the two spectrums in Figure 59 below.

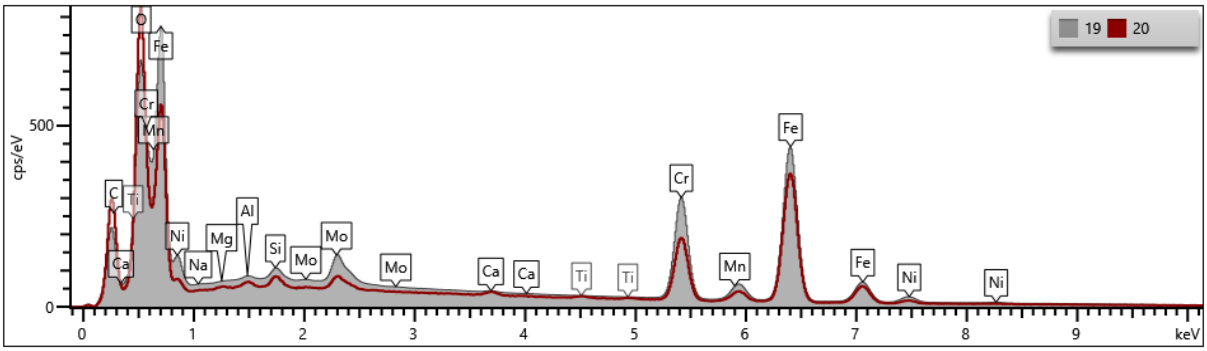

Figure 59: Spectrum 19 (grey) and 20 (red). Note the slightly higher C peak in spectrum 20.

7.4 Optimization of the Grinding Process

The primary difference between **Method 1** (current grinding method) and **Method 2** lies in the amount of material removed per processed slab. In the current method, both a coarse and fine pass are performed on both sides of each slab, resulting in a total grinding wheel material consumption of **44 mm per slab**. In contrast, Method 2 involves only a coarse pass on each side, reducing material consumption to **28 mm per slab**.

Figure 60: Grinding Wheel for Processing Slabs

Method 3 was excluded from the analysis because the combination of lower grinding speeds and higher pressures led to inconsistent material removal. As a result, the surface quality varied, making it unsuitable for direct comparison with Methods 1 and 2.

Below, the calculations for comparing Method 1 and the proposed Method 2 are presented. The calculations include material consumption, the number of slabs processed per grinding wheel, and the associated costs of the grinding process.

- **Total Available Abrasive Material for Grinding Wheel Wear:**
  Starting grinding wheel diameter: 610 mm
  Minimum grinding wheel diameter: 390 mm
  Total available material for grinding

$$610 - 390 = 220\ mm$$

  Abrasive Material Consumption per Slab (Grinding Wheel Wear):
  Method 1:

$$14mm\ (Rough - ground\ ) + 8mm\ (fine - ground) = 22\ mm$$

  Total Material Consumption per Slab:

$$22mm \times 2 = 44mm$$

  Method 2:

$$14mm\ (Rough - ground\ )$$

  Total Material Consumption per Slab:

$$14mm \times 2 = 28mm$$

  Number of Processed Slabs per Grinding Wheel:

Method 1:

Number of Slabs= $\frac{Total\ Available\ Material}{Material\ Consumption\ per\ Slab} = \frac{220}{44} = 5\ slabs$

Method 2:

Number of Slabs= $\frac{Total\ Available\ Material}{Material\ Consumption\ per\ Slab} = \frac{220}{28} \approx 7\ slabs$

- **Cost per Processed Slab:**
  Price per Grinding Wheel: 5000 SEK
  Method 1:
  Cost per Slab = $\frac{Price\ per\ Grinding\ Wheel}{Number\ of\ Processed\ Slabs} = \frac{5000}{5} = 1000\ sek/slabs$
  Method 2:
  Cost per Slab = $\frac{Price\ per\ Grinding\ Wheel}{Number\ of\ Processed\ Slabs} = \frac{5000}{7} = 714\ sek\ /slabs$

- **Total Cost for Processed Slabs from March 1, 2024, to June 15, 2024:**
  Number of processed slabs: 233
  Method 1:
  Number of grinding wheels required:

$$\frac{Number\ of\ Slabs}{Number\ of\ Slabs\ per\ Grinding\ Wheel} = \frac{233}{5} \approx 47\ PC$$

  Total cost: $47 \times 5000 = 235000\ kr$

  Method 2:
  Number of grinding wheels required:

$$\frac{Number\ of\ Slabs}{Number\ of\ Slabs\ per\ Grinding\ Wheel} = \frac{233}{7} \approx 34\ PC$$

  Total cost: $34 \times 5000 = 170000\ kr$

- **Cost Savings:**
  Savings per Slab:

$$1000 - 714 = 286\ sek.$$

  Total Savings:

$$235000 - 170000 = 65000\ sek.$$

- **Summary of the Calculation:**

Table 20: Comparison of Material Consumption Between Method 1 and Method 2.

	Method 1	Method 2	Difference
Abrasive Material Consumption per Slab	44 mm	28 mm	-36%
Number of Slabs per Grinding Wheel	5	7	+40%
Number of Grinding Wheels for 233 Slabs	47	34	-13 Grinding Wheels
Cost per Slab	1000	714	-29%
Total Cost (SEK)	235000	170000	-65 000 kr

By transitioning to **Method 2**, it is evident that both material and cost savings are achievable. The number of processed slabs per grinding wheel increases by **40%**, while the cost per processed slab decreases by **29%**. This implies that production becomes not only more efficient but also economically advantageous, particularly for larger volumes. In the long term, this method can contribute to a more sustainable and cost-effective production process.

7.5 Time and Material Savings

This section analyzes the differences in time and material consumption between the two grinding methods. Method 1 refers to the current grinding process, where both a coarse and a fine pass are performed on both sides of each slab. Method 2 refers to the proposed method, where only a coarse pass is performed on each side. The analysis is based on the processing of 233 slabs and aims to evaluate the differences in terms of time and material usage.

Figure 61: Slab after cold grinding.

When comparing time consumption and material loss between Method 1 and Method 2, significant differences become evident. For Method 1, the time required is 120 minutes and 59 seconds per slab. Converted into minutes, this is:

$$120 + {}^{59}/_{60} = 121\ Minutes\ per\ Slab.$$

For **Method 2**, the time required is **70 minutes and 26 seconds per slab**, which corresponds to:

$$70 + {}^{26}/_{60} = 71\ Minutes\ per\ Slab.$$

To calculate the total time required to process 233 slabs produced during the period from January 3 to June 15, we can use the time per slab for the two methods.

With Method 1:

$$121\ \times 233 \approx 28\ 181\ min\ \rightarrow\ {}^{28\ 181}/_{60} \approx 470\ h$$

With Method 2:

$$70\ \times 233 \approx 16\ 410\ min\ \rightarrow\ {}^{16\ 410}\ /_{60} \approx 274\ h$$

Time Savings:

$$28\ 181 - 16\ 410 = 11771\ min \rightarrow\ {}^{11\ 771}\ /_{60} \approx 196\ h$$

Material loss is a critical aspect of the grinding process, as it impacts both resource utilization and overall efficiency. To compare **Method 1** and **Method 2**, the total material loss during the processing of 233 slabs is evaluated.

With Method 1:
Material loss per slab: **410 kg**

$$410 \times 233 = 95\ 530\ kg$$

With Method 2:
Material loss per slab: **320 kg**.

$$320 \times 233 = 74\,560\ kg$$

Material Savings:

$$95\,530 - 74\,560 = 20970\ kg$$

Summary of the Calculation:

Table 21: Comparison of Time Consumption Between Method 1 and Method 2.

	Method 1	**Method 2**	**Difference**
Time per Slab (minutes)	121	70	-51 min
Total Time for 233 Slabs (hours)	470	274	-197 h
Material Loss per Slab (kg)	410	320	-90 kg
Total Material Loss (kg)	95 530	74 560	20 970 kg

Switching from Method 1 to Method 2 reduces the processing time per slab by 51 minutes, resulting in a total reduction of 197 hours for processing 233 slabs. Additionally, material loss per slab decreases by 90 kg, leading to a total savings of 20,970 kg for all slabs. The analysis clearly demonstrates that Method 2 is significantly more efficient in terms of both time and resources, making it a strong candidate for implementation in production. However, the surface after using Method 2 must be free from defects, just as for the standard Method 1 procedure.

7.6 Results from Cold Rolling:

In the study, several finished slabs were analyzed at the Cold Rolling Mill (KBR), and it was observed that only the slab processed using Method 2 was not scrapped. This result indicates that using Method 2 is not affecting the final surface quality negatively, although it is a small sample size.

The other materials were primarily scrapped due to scratches that occurred during the process in the hot rolling mill. See Figure 60.
While the results are promising and indicate potential improvements in grinding, further testing is required to ensure that the method performs reliably under varying conditions.

It is also important to note that some of the scrapping resulted from other stages in the process that were not directly related to surface quality. These factors made it more challenging to evaluate the results, but such difficulties are common in production trials. Addressing unforeseen issues is an integral part of optimizing the overall process.

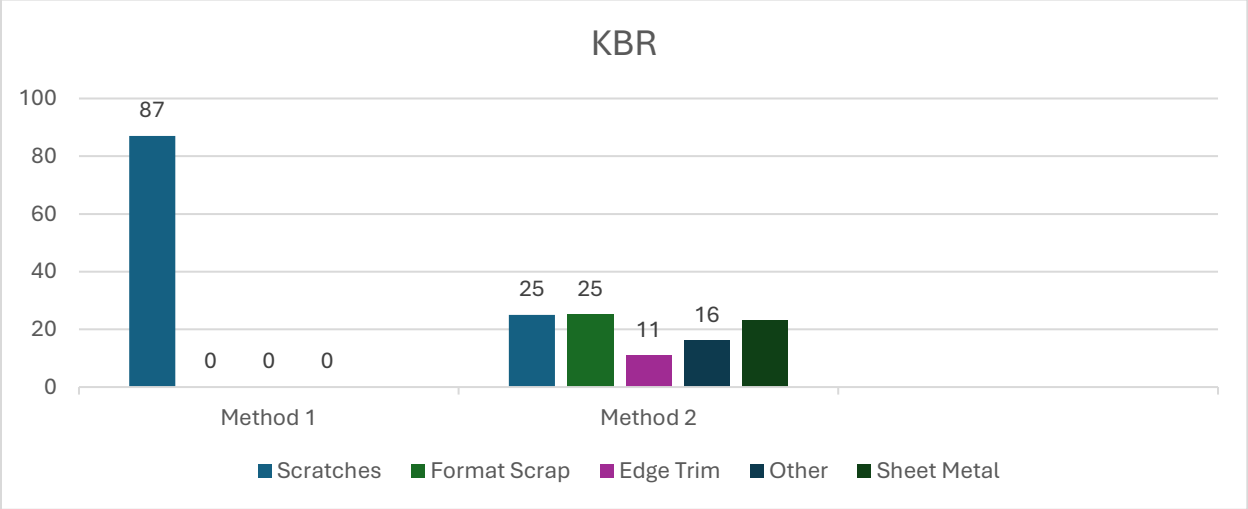

Figure 62: The Diagram Shows the Scrap Rate for the Two Different Methods

8 Discussion

This study has examined the possibilities for improving the grinding process of Duplex 2205 stainless steel. An important aspect was analyzing the oxide layers on the surface before and after grinding. The findings showed that grinding parameters significantly influence the thickness and structure of the oxide layers. These layers ranged from being homogeneous to more porous, depending on the settings. A smoother surface improves product quality and reduces the risk of defects, thereby decreasing the need for additional processing. It is therefore essential to tailor grinding parameters to the material's properties to achieve optimal results.

The focus was on analyzing and comparing two different methods to identify which is more efficient. The results indicate that Method 2 offers significant advantages over Method 1, both in terms of material savings and processing time. For 233 processed slabs, a material saving of 20,970 kg was achieved, while processing time was reduced by 196.37 hours. These results are based on actual measurements and include factors such as grinding wheel cost, labor costs, and process efficiency.

The study also demonstrated that optimized parameters, such as grinding wheel pressure, speed, and angle, not only enhance surface quality but also reduce wear on grinding wheels. This leads to longer equipment lifespans and a more sustainable production process. Improved process control also minimizes energy consumption and reduces material waste, which is beneficial both economically and environmentally.

Another important finding is how an optimized grinding process can strengthen the company’s ability to meet customer demands. The precision and flexibility of grinding are crucial for producing steel products with the correct specifications and high quality. By reducing costs and improving productivity, the company can also create a more competitive manufacturing process.

Oxide/casting powder can be found in the bulk material, meaning that it is often necessary to remove some amount of material on the surface, not only the outmost oxide layer. This oxide/casting powder can lead to surface defects on the finished coil.

9 Conclusions

- Current Hot Ground Surfaces: Produced slabs exhibit a roughness of $R_a$between $10.6 - 14.4\ \mu m$ and R_z between $42.0 - 95.6\ \mu m$. The R_a (average surface roughness) is $10.78\ \mu m$ and R_z (average maximum surface roughness) is $72.14\ \mu m$.
- Current Cold Ground Surfaces: Produced slabs exhibit a roughness Ra between 6.6−15.5 μm with an average of 11.13 μm. and R_z between $38.7 - 98.6\ \mu m$ with an average of $64.58\ \mu m$
- Method Comparison: R_a and R_z values differed between Methods 1, 2, and 3. Method 2 provided a sufficiently good surface quality to be considered for implementation.
- Surface Layer Analysis: Un-ground slabs primarily consisted of elements such as Ca and Na.
- Traces of Casting Powder: Traces were found on hot-ground surfaces but were not present after cold grinding.
- Efficiency of Method 2: If Method 2 is implemented, savings of up to 200 hours could be achieved, and grinding wheel costs could be reduced by 40% within the reference period.
- Material Savings with Method 2: By implementing Method 2, the total material loss can be reduced by 20,970 kg, contributing to significant cost and resource efficiency improvements.
- Post-Processing Results: Results after cold rolling in KBR were mostly inconclusive.
- Presence of Oxide/Casting Powder: Oxide/casting powder can be found in the bulk material. This oxide/casting powder can lead to surface defects on the finished coil.

10 Suggestions for future work

This study has demonstrated significant potential for improving the grinding process of Duplex 2205 stainless steel, though several areas remain for further development and investigation. To ensure the scalability of the study's results, it is essential to conduct additional tests and evaluations.

A crucial first step is to apply Method 2 to a larger number of slabs under varying conditions. By processing more slabs and sending them to the Cold Rolling Mill (KBR), the method's stability and potential can be verified. Such tests would provide a better understanding of how the method affects the quality of the final product under different production environments and settings.

Another area for future research is to explore whether the method can be adapted to other materials. So far, the study has focused on Duplex 2205 stainless steel, but the potential to use optimized parameters on other steel grades and alloys should be examined. Conducting tests on various materials would allow for the development of specific guidelines, facilitating the adaptation of the process to meet diverse customer needs and production requirements.

To further enhance the grinding process, it would be valuable to investigate how different combinations of pressure, speed, and feed rates affect the results. A practical way to conduct this research is to use slabs already designated for scrapping. This approach allows for testing more extreme settings without risking the quality of products intended for use. By experimenting with different parameters, the optimal settings for achieving a smooth and high-quality surface can be identified. Simultaneously, the effects of these parameters on machine wear and energy consumption can be evaluated. The goal is to achieve a balance where surface quality improves without a significant increase in operational costs.

Finally, it is essential to test the improved methods in large-scale production environments. This will provide a clearer understanding of how the changes impact the entire production chain and how they can be practically and economically implemented.

In conclusion, this study identifies several promising paths forward. By building on the results, the company can not only improve its productivity and quality but also contribute to a more sustainable and efficient manufacturing industry.

11 References

1. History of Outokumpu. (n.d.). Outokumpu. https://www.outokumpu.com/en/about-outokumpu/history-of-outokumpu
2. Outokumpu Avesta handbok 2013SE.1. August 2018 (13:15 19/08/2024)
3. Duplex stainless-steel grades | High strength and corrosion resistance. (n.d.). Outokumpu. https://www.outokumpu.com/en/products/stainless-steel-types/duplex-stainless-steel?gad_source=1&gbraid=0AAAAD9c4WyyhHCM8-5TceTkEnUMi-UvY&gclid=CjwKCAjw59q2BhBOEiwAKc0ijXfCB6K8sxlTdsUQ_RCZmJztnt1PX9xg7KiuTBqRIZvE-ouqAaJathoCPUwQAvD_BwE
4. Cleland, J. (1996). What does the pitting resistance equivalent really tell us? Engineering Failure Analysis, 3(1), 65–69. https://doi.org/10.1016/1350-6307(95)00026-7
5. Penn Stainless Products. (2019, February 4). Duplex 2205 Stainless Steel - Penn Stainless. Penn Stainless. https://www.pennstainless.com/resources/product-information/stainless-grades/duplex-grades/duplex-2205-stainless-steel/
6. Handbook of stainless steel, Outukumpu high performance stainless steel.
7. Punktkorrosion. (n.d.). Hitta Leverantör, Metod & Material. https://www.manufacturingguide.com/sv/ordlista/punktkorrosion
8. Hed, M. (2022, November 1). De fem huvudgrupperna inom rostfritt stål. Snacka om rostfritt - Allt om rostfritt stål. https://snackaomrostfritt.se/allmant-om-rostfritt/de-fem-huvudgrupperna-inom-rostfritt-stal/
9. ESAB Europe. (2021, October 21). How to Weld Duplex Stainless Steels, and Why They are So Good. [Video]. YouTube. https://www.youtube.com/watch?v=zrX3FbB-3K0
10. Principles of Modern Grinding Technology. (n.d.). ScienceDirect. https://www.sciencedirect.com/book/9780323242714/principles-of-modern-grinding-technology
11. Ye, R. (2024, March 13). What is Grinding: Definition, Process, Types & Specifications. Rapid Prototyping & Low Volume Production. https://www.3erp.com/blog/what-is-grinding/
12. ABM Proceedings - Pagina inicial. (n.d.). https://abmproceedings.com.br/ptbr/article/download-pdf/mais-recentes-desenvolvimentos-para-condicionamentosuperficial-de-placas-inovao-em-esmerilhamento-de-placas-2&ved=2ahUKEwi0mK3-zMWIAxUbHhAIHajMD88QFnoECBQQAQ&usg=AOvVaw2TQ4In0Ki67aOwihTw7NEZ
13. Jarfors, Carlsson, Eliasson, Keife, Nicolescu, Rundqvist, Bejhem, Sandberg. *Tillverkningsteknologi*.Stockholm juni, 2010.
14. Rundslipning. (n.d.). Hitta Leverantör, Metod & Material. https://www.manufacturingguide.com/sv/rundslipning
15. Various grinding methods | A.L.M.T. Corp. (n.d.). https://www.allied-material.co.jp/en/products/diamond/knowledge/various_grinding.html
16. Norton. (n.d.). Allmänt om slipskivor. In STEP System IMAGE2. https://foretagsshop.skenejarn.se/Doc/110/00/1100023.pdf
17. Hard Machining Course, s.l. : SKF, September 2015.

18. Machining, Cutting & Grinding Stainless Steel|Outokumpu Stainless steel. (n.d.). Outokumpu. https://www.outokumpu.com/en/expertise/stainless-basics/machining-and-cutting-and-grinding
19. Hot rolled stainless steel coil, strip and plate. (n.d.). Outokumpu. https://www.outokumpu.com/en/products/flat-products/hot-rolled-coil-strip-and-plate
20. Hou, Z. B., & Komanduri, R. (2003). On the mechanics of the grinding process – Part I. Stochastic nature of the grinding process. International Journal of Machine Tools and Manufacture, 43(15), 1579–1593. https://doi.org/10.1016/s0890-6955(03)00186-x
21. Tawakoli, T., Reinecke, H., & Vesali, A. (2012). An Experimental Study on the Dynamic Behavior of Grinding Wheels in High Efficiency Deep Grinding. Procedia CIRP, 1, 382–387. https://doi.org/10.1016/j.procir.2012.04.068
22. Tom R. Thomas (Production Engineering Department), Rough Surfaces, Second Edition. Chalmers University of Technology, First published 1999.
23. What is surface roughness? | Introduction to roughness | Introduction to roughness | KEYENCE America. (n.d.). https://www.keyence.com/ss/products/microscope/roughness/line/
24. Dobes, J., Leal, J. E. S., Profeta, J., De Sousa, M. M., Neto, F. P. L., Piratelli-Filho, A., & Arencibia, R. V. (2017). Effect of mechanical vibration on Ra, Rq, Rz, and Rt roughness parameters. The International Journal of Advanced Manufacturing Technology, 92(1–4), 393–406. https://doi.org/10.1007/s00170-017-0137-0
25. Arithmetical Mean Height (RA, PA, WA) | Surface Roughness Parameters | Introduction to Roughness | KEYENCE America. (n.d.). https://www.keyence.com/ss/products/microscope/roughness/line/parameters.jsp
26. Maximum Height Of Profile (Rz, Pz, Wz) | What Is Line Roughness? | Introduction To Roughness | KEYENCE America. (n.d.). https://www.keyence.com/ss/products/microscope/roughness/line/maximum-height-of-profile.jsp
27. Total Height Of Profile (Rt, Pt, Wt) | Surface Roughness Parameters | Introduction To Roughness | KEYENCE America. (n.d.). https://www.keyence.com/ss/products/microscope/roughness/line/total-height-of-profile.jsp
28. Sandvik Coromant. (n.d.). Sandvik Coromant. https://www.sandvik.coromant.com/en-us/knowledge/materials/workpiece-surface-measurement
29. Ytjämnhetsmätare SJ210, Typ: SJ210 | Hoffmann Group. (n.d.). https://www.hoffmann-group.com/SE/sv/ravema/p/499205-SJ210
30. ANCA. (2011). *Aggressiveness – A better way to set speeds and feeds for tool grinding*. ANCA CNC Machines. Aggressiveness - A Better Way to Set Speeds and Feeds for Tool Grinding - ANCA - CNC Machines
31. Graf, W. (2020). *Surface Grinding's Aggressiveness Factor Fa*. LinkedIn. Hämtad från: Surface Grinding's Aggressiveness Factor Fa
32. ANCA. (2011). *A Better Way to Set Speeds and Feeds for Tool Grinding*. ANCA Machines. Hämtad från:

Aggressiveness - A Better Way to Set Speeds and Feeds for Tool Grinding - ANCA - CNC Machines

Appendix

This appendix includes a table listing the chemical notations referenced in this thesis. The table is intended to offer a clear overview of the notations and their meanings, making it easier to follow and understand the content.

Chemical Notation	Full Name
C	Carbon
O	Oxygen
N	Nitrogen
Cr	Chromium
Ni	Nickel
Mg	Magnesium
Mn	Manganese
Mo	Molybdenum
Fe	Iron
Na	Sodium
Al	Aluminum
Si	Silicon
Ca	Calcium

DEPARTMENT OF INDUSTRIAL AND MATERIALS SCIENCE
CHALMERS UNIVERSITY OF TECHNOLOGY
Gothenburg, Sweden 2025
www.chalmers.se

CHALMERS
UNIVERSITY OF TECHNOLOGY